

## ON THE AMPLITUDE OF CONVECTIVE VELOCITIES IN THE DEEP SOLAR INTERIOR

MARK S. MIESCH<sup>1</sup>, NICHOLAS A. FEATHERSTONE<sup>1</sup>, MATTHIAS REMPEL<sup>1</sup> AND REGNER TRAMPEDACH<sup>2</sup><sup>1</sup>High Altitude Observatory, National Center for Atmospheric Research, Boulder, CO, 80307-3000, USA: miesch@ucar.edu and<sup>2</sup>JILA, University of Colorado and National Institute of Standards and Technology, 440 UCB, Boulder, CO 80309*Draft version March 3, 2013*

## ABSTRACT

We obtain lower limits on the amplitude of convective velocities in the deep solar convection zone based only on the observed properties of the differential rotation and meridional circulation together with simple and robust dynamical balances obtained from the fundamental MHD equations. The linchpin of the approach is the concept of gyroscopic pumping whereby the meridional circulation across isosurfaces of specific angular momentum is linked to the angular momentum transport by the convective Reynolds stress. We find that the amplitude of the convective velocity must be at least  $30 \text{ m s}^{-1}$  in the upper CZ ( $r \sim 0.95R$ ) and at least  $8 \text{ m s}^{-1}$  in the lower CZ ( $r \sim 0.75R$ ) in order to be consistent with the observed mean flows. Using the base of the near-surface shear layer as a probe of the rotational influence, we are further able to show that the characteristic length scale of deep convective motions must be no smaller than 5.5–30 Mm. These results are compatible with convection models but suggest that the efficiency of the turbulent transport assumed in advection-dominated flux-transport dynamo models is generally not consistent with the mean flows they employ.

## 1. INTRODUCTION

Our modern understanding of solar internal dynamics rests heavily on global and local helioseismology, with perspective provided by theoretical and numerical models. This perspective is particularly important in the deepest regions of the convection zone where mean flows are established and where helioseismic probing is most challenging.

The most reliable result from helioseismology with regard to the dynamics of the deep convection zone (CZ) continues to be the solar internal rotation profile obtained from global inversions (Thompson et al. 2003). Such inversions indicate that the monotonic surface differential rotation ( $\sim 30\%$  decreases in angular velocity  $\Omega$  from equator to pole) persists throughout the convection zone with little radial variation. Further dynamical clues come from estimates of the meridional flow near the surface inferred from local helioseismic inversions and photospheric observations (González-Hernández et al. 2006; Basu & Antia 2010; Ulrich 2010; Hathaway & Rightmire 2010; Hathaway 2011). Although various measurement techniques can yield disparate results for the radial and temporal dependence of the meridional flow, all techniques generally agree that there is a persistent poleward flow near the surface ( $r \gtrsim 0.95R$ , where  $R$  is the solar radius) from the equator up to latitudes of at least  $60\text{--}70^\circ$ , with an amplitude of  $10\text{--}20 \text{ m s}^{-1}$ .

Less is known about the structure or amplitude of convective flows in the deep convection zone. Photospheric observations are dominated by solar granulation, with a velocity scale of  $\sim 2 \text{ km s}^{-1}$  and a size scale of  $\sim 1\text{Mm}$ , but deep convective motions are thought to be much slower and larger (e.g. Miesch & Toomre 2009). Closer scrutiny of the photospheric velocity power spectrum obtained from Doppler measurements shows a prominent peak near a spherical harmonic degree  $\ell \sim 120$ , corresponding to a size scale of 30–35 Mm and a spectral velocity amplitude of  $7\text{--}8 \text{ m s}^{-1}$  (Hathaway et al. 2000).

However, this observed spectral amplitude is significantly lower than the true amplitude of the convection due mainly to projection effects; the Doppler measurements trace mainly horizontal flows near the limb. Taking projection and other sampling effects into account (e.g. spatial and temporal filtering), Hathaway et al. were able to match the observed spectrum near  $\ell \sim 120$  with a supergranular flow component having a typical velocity amplitude of about  $300\text{--}400 \text{ m s}^{-1}$ , in agreement with the correlation tracking of surface features (DeRosa & Toomre 2004; Roudier et al. 2012). The power declines steadily toward lower  $\ell$ , where one would expect to see signatures of deep convection (giant cells). Thus, either giant cells have a lower amplitude than supergranulation, or they do not imprint through to the photosphere (or both).

Hanasoge et al. (2010, 2012) have recently searched for signatures of subsurface convection in local helioseismic inversions at depths of  $0.92R$ ,  $0.95R$ , and  $0.96R$ . Their analysis indicates that the spectral velocity amplitude at these depths is less than  $10 \text{ m s}^{-1}$  and possibly less than  $1 \text{ m s}^{-1}$  for convective motions with  $\ell < 60$  and correlation times longer than 96 hours. This is one to two orders of magnitude lower than suggested by convection simulations and mixing length theory (see §4.2).

In this paper we argue that these results, if confirmed, would have important implications for the maintenance of mean flows in the Sun. In particular, we use fundamental physical arguments together with solar observations to derive lower bounds on the amplitude of convective motions in the deep solar interior. These estimates are based on robust dynamical balances deduced from the equations of magnetohydrodynamics (MHD). They are not based on mixing length theory and they do not depend on any results from numerical simulations, although they are consistent with both (§4.2). We find that the amplitude of convective motions in the upper convection zone ( $r \sim 0.95$ ) must be at least  $30 \text{ m s}^{-1}$  in order to be capable of sustaining the mean flows inferred from helioseismology. Similar estimates for the lower CZ

( $r \sim 0.75R$ ) imply that convective motions there must be at least  $8 \text{ m s}^{-1}$ . Reconciling these lower limits with the upper limits found by Hanasoge et al. (2010, 2012) is a challenge for global convection models but may be possible if the motions responsible for maintaining mean flows span multiple scales, with significant power above  $\ell \sim 60$ .

In §2 we discuss how differential rotation and meridional circulation are maintained in the Sun by means of the convective Reynolds stress, baroclinicity, and their own inertia. This provides a link between convection and mean flows that we exploit in §3 to obtain lower limits on the amplitude of convective motions in the deep convection zone. In §4 we address the length scale of convective motions and the implications of our velocity and length scale estimates for helioseismic probing, flux-transport dynamo models, and convection models. Section 5 is a summary of our principle results and conclusions.

## 2. CONVECTIVE ORIGINS OF MEAN FLOWS

### 2.1. Gyroscopic Pumping

The conservation of angular momentum for a statistically steady flow in a rotating spherical shell may be expressed as follows (Miesch & Hindman 2011, hereafter MH11):

$$\langle \rho \mathbf{v}_m \rangle \cdot \nabla \mathcal{L} = \mathcal{F} \quad . \quad (1)$$

where  $\rho$  is the mass density,  $\mathcal{L} = \lambda^2 \Omega$  is the specific angular momentum,  $\Omega$  is the rotation rate,  $\lambda = r \sin \theta$  is the cylindrical radius, and  $\langle \mathbf{v}_m \rangle = \langle v_r \rangle \hat{\mathbf{r}} + \langle v_\theta \rangle \hat{\boldsymbol{\theta}}$  is the mean meridional flow. This equation is derived by averaging the zonal momentum equation over longitude and time, with averages denoted by angular brackets  $\langle \rangle$ . Spherical polar coordinates ( $r, \theta, \phi$ ) are used throughout.

The  $\mathcal{F}$  term in eq. (1) is a net axial torque that includes contributions from the Reynolds stress, the Lorentz force, and the viscous diffusion. Explicit expressions are given in MH11. The molecular viscosity is small in stars so viscous diffusion can be safely neglected. Neglecting the Lorentz force is less justified. However, the magnetic pressure gradient averages out when taking the mean so the only contribution of the Lorentz force to  $\mathcal{F}$  is from magnetic tension. This generally tends to suppress rotational shear (e.g. Brun et al. 2004) so it is unlikely to be the dominant factor in establishing the solar differential rotation. In this paper we wish to establish a lower limit on how strong the Reynolds stress must be in order to balance the advection of angular momentum by the meridional flow; that is, the term on the left-hand-side (LHS) of (1). If it must also balance magnetic tension, then the Reynolds stress must be even stronger. Therefore, the inclusion of the Lorentz force is not likely to change the lower bounds we establish in §3.

Thus, if we assume the Reynolds stress is the dominant contribution to  $\mathcal{F}$ , Eq. (1) becomes

$$\langle \rho \mathbf{v}_m \rangle \cdot \nabla \mathcal{L} = -\nabla \cdot (\langle \rho \lambda \mathbf{v}'_m v'_\phi \rangle) \quad . \quad (2)$$

where primes indicate fluctuations about the mean. Since  $\nabla \mathcal{L}$  is cylindrically outward in the Sun, the implication here is that the angular momentum transport by the Reynolds stress (RHS) establishes the meridional flow by inducing a flow toward the rotation axis when the RHS is negative (divergence) and away from the

rotation axis when the RHS is positive (convergence). This mechanism is known as gyroscopic pumping (MH11; McIntyre 1998) and is supported by convection simulations and mean-field models (Rempel 2005; Brun et al. 2011; Featherstone et al. 2012).

The fundamental physics behind gyroscopic pumping is discussed by MH11, Haynes et al. (1991) and McIntyre (1998). In short, an axial variation in the net torque  $\partial \mathcal{F} / \partial z$  establishes an axial shear  $\partial \Omega / \partial z$  which in turn induces a meridional flow through the Coriolis force (§2.2). In order to determine the nature of the differential rotation that will ultimately be established, one must consider the meridional force balance as we do in the next section. However, the equilibrium structure of the meridional flow is surprisingly less sensitive to the meridional force balance and is instead regulated mainly by eq. (1). This is because the primary contribution to  $\nabla \mathcal{L}$  is from the mean (globally averaged) rotation rate of the Sun,  $\Omega_0$  (see MH11 and §3.2 below), so changes in the differential rotation,  $\nabla \Omega$ , do not change the balance in eq. (1) appreciably.

### 2.2. Meridional Force Balance and the Role of Baroclinicity

In §2.1 we argued that the mean meridional circulation in the solar envelope is established and maintained through gyroscopic pumping, as expressed by eq. (1). Since the process of gyroscopic pumping is mediated by the Coriolis force, this is equivalent to saying that the meridional circulation is maintained by the inertia of the differential rotation (MH11). However, it is well known that thermal gradients can also establish meridional circulation by means of baroclinicity and it is sometimes argued that the meridional flow in the solar convection zone may be baroclinic in nature. In this section we argue that this is not the case. In particular, we consider the meridional force balance in the solar convection zone within the context of solar observations and we argue that gyroscopic pumping, as expressed in eq. (1), rather than baroclinicity, is the primary mechanism by which the solar meridional circulation is maintained.

The ambiguity arises because the thermal energy equation can be expressed in a manner analogous to eq. (1):

$$\langle \rho \mathbf{v}_m \rangle \cdot \nabla \langle S \rangle = \mathcal{Q} \quad . \quad (3)$$

where  $\mathcal{Q}$  involves the (negative) divergence of the convective entropy flux, the radiative diffusion, and the viscous and ohmic heating, although the latter are negligible in stellar interiors.

It is clear from equations (1) and (3) that both mechanical and thermal forcing,  $\mathcal{F}$  and  $\mathcal{Q}$ , can induce a meridional circulation. Indeed, this is a classical problem in the theory of planetary and stellar atmospheres (Eliassen 1951; Read 1986; Tassoul 1978). In a solar context, eq. (3) plays an important role in the radiative spreading of the solar tachocline (Spiegel & Zahn 1992).

We can be reasonably certain from solar observations that both  $\mathcal{F}$  and  $\mathcal{Q}$  are nonzero. If this were not the case, then a steady state would only be possible if either  $\mathcal{L}$  or  $\langle S \rangle$  were constant on streamlines of the meridional mass flux. Helioseismic rotational inversions together with observations of poleward mass flux in the solar surface layers rule out the former ( $\mathcal{L}$  constant on streamlines). The

latter is ruled out by mass conservation ( $\langle v_r \rangle$  must be nonzero in the deep convection zone to sustain the poleward mass flux in the surface layers) and the requirement that at least some portion of the convection zone be superadiabatic  $\partial \langle S \rangle / \partial r < 0$ .

The relative contribution of mechanical and thermal forcing to establishing the meridional flow becomes more clear if we consider the mean zonal vorticity equation (e.g. Miesch 2005; Balbus et al. 2009, MH11). This is obtained from the meridional components of the MHD momentum equation, averaged over longitude and time. Previous work based on numerical convection simulations (Brun & Toomre 2002; Miesch et al. 2006), mean-field models (Kitchatinov & Rüdiger 1995; Rempel 2005), and theoretical interpretation of helioseismic rotational inversions (Balbus et al. 2009) suggest that the dominant contributions to this equation are the Coriolis and centrifugal terms associated with the differential rotation as well as the zonal component of the baroclinic vector. The latter is proportional to the mean latitudinal entropy gradient if the stratification is nearly hydrostatic and adiabatic and if the equation of state is that of an ideal gas. Thus, neglecting the meridional components of the Reynolds stress, the Lorentz force, the viscous diffusion, thermal fluctuations, and quadratic terms in  $\langle \mathbf{v}_m \rangle$  yields

$$\frac{\partial}{\partial t} \langle \omega_\phi \rangle = \lambda \frac{\partial \Omega^2}{\partial z} - \frac{g}{r C_P} \frac{\partial \langle S \rangle}{\partial \theta} \quad , \quad (4)$$

where  $\omega_\phi$  is the longitudinal component of the fluid vorticity  $\boldsymbol{\omega} = \nabla \times \mathbf{v}$ ,  $S$  is the specific entropy,  $g$  is the gravitational acceleration, and  $C_P$  is the specific heat at constant pressure.

We have retained the time dependence in eq. (4) in order to illustrate how mechanical and thermal forcing influence the evolution of the meridional flow. If the balance in equation (1) is not satisfied, this will lead to a change in the specific angular momentum  $\partial \mathcal{L} / \partial t = \lambda^2 \partial \Omega / \partial t$  that will in turn influence the meridional flow through the first term on the RHS of eq. (4). Likewise, any imbalance in equation (3) will change the baroclinic (second) term through  $\partial \langle S \rangle / \partial t$ .

The system will evolve nonlinearly toward thermal wind balance (TWB), described by an equation that is now well known:

$$\frac{\partial \Omega^2}{\partial z} = \frac{g}{r \lambda C_P} \frac{\partial \langle S \rangle}{\partial \theta} \quad . \quad (5)$$

Most current theoretical and numerical models of solar mean flows attribute the conical nature of the solar differential rotation profile ( $\partial \Omega^2 / \partial z \neq 0$ ) to latitudinal entropy gradients through eq. (5). In particular, Balbus et al. (2009) have argued that the orientation of the  $\Omega$  isosurfaces in the solar CZ inferred from helioseismology follows from thermal wind balance, Eq. (5), together with the hypothesis that isorotation and isentropic surfaces coincide. Furthermore, the existence of the near-surface shear layer suggests that there is a transition near  $r \sim 0.95R$  below which the Rossby number is less than unity and thermal wind balance prevails (MH11).

Although we agree that it plays an essential role in determining the orientation of the angular velocity isosurfaces in the solar convection zone, we note that baro-

clincity due to axisymmetric thermal gradients cannot account for the existence of the solar differential rotation. The zonal component of the Reynolds stress must also contribute. This is demonstrated in the Appendix.

Here we wish to focus on the approach to thermal wind balance by means of the time-dependent vorticity equation (4). Although the meridional circulation itself, represented by  $\langle \omega_\phi \rangle$ , drops out of the balance equation in a steady state, any imbalance between the inertial and baroclinic terms on the RHS will induce a flow. Consider for example the northern hemisphere (NH). There it is well known from helioseismic observations that  $\partial \Omega^2 / \partial z < 0$  (Thompson et al. 2003). This will tend to induce a counter-clockwise (CCW) circulation ( $\langle \omega_\phi \rangle < 0$ , poleward in the upper convection zone) that will act to make the  $\Omega$  profile more cylindrical ( $\partial \Omega / \partial z = 0$ ) in accordance with the Taylor-Proudman theorem. In order to oppose this and achieve TWB [Eq. (5)], there must be a poleward entropy gradient ( $\partial \langle S \rangle / \partial \theta < 0$  in the NH). In short, the inertial term tends to induce a CCW circulation in the northern hemisphere while the baroclinic term tends to induce a clockwise (CW) circulation (vice versa in the southern hemisphere).

In the approach to equilibrium, one of these terms must act as the driver, accelerating the meridional flow, while the other acts as a resistance, opposing the acceleration until a balance is achieved. The observed poleward sense of the meridional flow near the solar surface (§1) indicates that the driver is in fact the inertial term  $\propto \partial \Omega / \partial z$ . As demonstrated in §2.1, this links the mean flows directly to the convective Reynolds stress and enables us to estimate the amplitude of the convective velocities based on the observed differential rotation and meridional flow.

There is one potential caveat to this conclusion. The recent analysis by Hathaway (2011) based on autocorrelation of photospheric Dopplergrams suggests that there may be a reversal of the meridional flow at  $r \sim 0.95R$ . If this is indeed true, then we cannot rule out a CW circulation cell (NH, CCW in the south) in the deep convection zone driven by baroclinic forcing (implying poleward flow near the base of the CZ). However, this is in conflict with helioseismic inversions which suggest the meridional flow remains poleward well below  $0.95R$  (Giles et al. 1997; Braun & Fan 1998; Chou & Dai 2001; Beck et al. 2002). Furthermore, poleward flow near the base of the CZ would be disastrous for flux-transport dynamo models (§4.3). This in itself does not preclude the presence of such a cell but it demonstrates that poleward flow at the base of the convection zone is contrary to our current understanding of solar interior dynamics.

### 3. AMPLITUDE OF CONVECTIVE VELOCITIES

#### 3.1. Fundamental Expressions

In this section we use Eq. (2) to obtain lower limits on the amplitude of convective velocities throughout the solar convection zone. The motions we are most interested in are the motions that are responsible for establishing the solar differential rotation by means of the Reynolds stress. Thus, unlike solar granulation, they must be large enough and slow enough to sense the rotational influence and spherical geometry. The mere existence of the solar differential rotation is evidence for the presence of such motions. In what follows, we will quantify what we mean

by *large enough* and *slow enough*.

We begin by estimating the amplitude of the Reynolds stress inside the divergence operator on the RHS of Eq. (2);

$$\langle \rho \lambda \mathbf{v}'_m v'_\phi \rangle \sim \rho \lambda \epsilon V_c^2 \quad (6)$$

where  $V_c$  is the characteristic amplitude of the convective velocity and  $\epsilon = \left| \langle v'_\phi \mathbf{v}'_m \rangle \right| V_c^{-2}$  is a correlation coefficient describing the efficiency of the convective angular momentum transport. If flows are perfectly correlated, the transport is efficient and  $\epsilon = 1$ . However, in practice  $\epsilon$  will fall somewhere between zero and one. Convection simulations such as that shown in Fig. 4 below yield  $\epsilon \sim 0.1$ – $0.2$ . Similar values of  $\epsilon$  are given by the mean-field theory of Kitchatinov & Rüdiger (2005). There the amplitude of the non-diffusive component of the Reynolds stress,  $\Lambda$ , is of order  $\nu_t \Omega_0 \mathcal{H}$  where  $\nu_t \sim V_c^2 \tau_c / 3$  is the turbulent viscosity,  $\tau_c$  is the correlation time, and  $\mathcal{H}$  is a nondimensional normalization factor that depends on the inverse Rossby number  $\Omega^* = 2\tau_c \Omega_0$ . This yields  $\epsilon \sim \Lambda V_c^{-2} \sim \Omega^* \mathcal{H} / 6$ , which according to their model, is about 0.1–0.2 in the lower CZ.

Note that we use a single velocity scale  $V_c$  to characterize the convection but this does not necessarily imply that the velocity field is isotropic. On the contrary, the velocity scale is defined in terms of the Reynolds stress through equation (6), which requires some degree of anisotropy. Thus,  $V_c$  can be regarded in general as the geometric mean of the two velocity components that dominate the Reynolds stress.

Throughout the paper we assume that the density  $\rho$  is spherically symmetric and is approximately given by Model S of Christensen-Dalsgaard et al. (1996). Then substituting (6) into (2) and noting that  $0 \leq \epsilon \leq 1$  provides a lower limit on  $V_c$

$$V_c \sim \left( \frac{\delta}{\epsilon} V_m |\nabla \mathcal{L}| \right)^{1/2} \gtrsim (\delta V_m |\nabla \mathcal{L}|)^{1/2} \quad (7)$$

where  $V_m$  is a characteristic amplitude of the meridional flow and  $\delta = L_t / \lambda$  where  $L_t$  is the length scale associated with the divergence operator in (2) and  $\lambda = r \sin \theta$  as above.

As above with the convection, we emphasize that the meridional flow is not isotropic. This is particularly true in the upper and lower boundary layers of the CZ where the meridional flow is predominantly horizontal and at the equator where it is predominantly vertical. The proper interpretation for  $V_m$  is the amplitude of the flow across  $\mathcal{L}$  isosurfaces, which are approximately cylindrical. So,  $V_m$  should be regarded as the flow toward or away from the rotation axis, which may be predominantly radial or latitudinal depending on the latitude.

A useful variation of equation (7) can be obtained if we consider only the component of  $\mathcal{L}$  involving the mean rotation rate  $\Omega_0$ . This gives  $|\nabla \mathcal{L}| \sim 2V_\Omega$  where  $V_\Omega = \lambda \Omega_0$  is the zonal velocity associated with the rotation of the star. Substituting this into Eq. (7) gives

$$V_c \gtrsim (2\delta V_m V_\Omega)^{1/2} \quad (8)$$

Thus, if  $(2\delta)^{1/2}$  is of order unity, then a lower limit on the convective velocity can be obtained by taking the geometric mean between the meridional flow speed and

the rotational speed, relative to an inertial frame. Taking nominal values of  $V_m \sim 2$ – $10$  m s<sup>-1</sup>,  $\Omega_0 = 2.7 \times 10^{-6}$  s<sup>-1</sup>, and  $\lambda \sim 0.85 R / \sqrt{2}$  would then yield  $V_c \gtrsim 47$ – $106$  m s<sup>-1</sup>. However, as we will see below,  $(2\delta)^{1/2}$  is likely to be somewhat less than unity, bringing these estimates down. Still, the extension from (7) to (8) is robust, since the differential rotation serves to steepen the  $\mathcal{L}$  gradient relative to the uniform rotation value of  $2V_\Omega$  (see §3.2).

It now remains to estimate  $\delta$ . In this context, it is important to emphasize that  $L_t$  reflects the scale of turbulent transport, which is not necessarily the same as the scale  $L_c$  of the convective motions themselves (the latter is addressed in §4.1). If the balance expressed by Eq. (2) is to be realized, then this scale must be intimately linked to the structure of the meridional circulation. Indeed, if our picture of gyroscopic pumping is correct then the structure of the meridional circulation is largely *determined* by the spatial variation of the Reynolds stress, as reflected by  $L_t$ .

To illustrate this relationship, consider the simplest case of a single meridional circulation cell in each hemisphere, with poleward flow in the upper CZ and equatorward flow in the lower CZ. Then the LHS of Eq. (2) would be correspondingly negative and positive in the upper and lower CZ respectively. To balance this, the RHS must also change sign, suggesting  $L_t \sim D/2$ , where  $D$  is the depth of the convection zone. If  $\mathcal{F}$  were to exhibit multiple sign changes across the CZ, this would produce multiple layered circulation cells in radius such that  $L_t \sim D/(2N_c)$  where  $N_c$  is the number of cells. For the moment arm we can consider mid-latitudes in the mid-convection zone, so  $\lambda \sim r_m / \sqrt{2}$ , where  $r_m \sim 0.85 R$ . Thus, we have

$$\delta = \frac{\sqrt{2} L_t}{r_m} \sim \frac{D}{\sqrt{2} r_m N_c} \sim \frac{0.25}{N_c} \quad (V_m = |\langle v_\theta \rangle| \text{ at } 45^\circ \text{ lat}) \quad (9)$$

where we have used the value for the Sun of  $D/R \sim 0.3$ . As noted, this corresponds to poleward or equatorward flow at mid latitudes in one or more circulation cells. So, when used with Eq. (7) or (8) the value of  $V_m$  should correspond to the latitudinal flow speed.

The caveat that can potentially limit the applicability of eq. (9) is that, although  $N_c$  is regulated by the number of nodes in  $\mathcal{F}$  (sign changes in the Reynolds stress divergence), the flow amplitude  $V_m$  is regulated by local gradients. This is particularly important at the base of the CZ where a strong convergence of the angular momentum flux over a narrow layer could drive an arbitrarily strong equatorward flow  $V_m$  for a given  $V_c$ .

To demonstrate this concept, consider a single-celled meridional circulation profile ( $N_c = 1$ ) as illustrated in Figure 1. We define the radius  $r_0$  as the turnaround radius, where the poleward flow in the upper CZ transitions to the equatorward flow in the lower CZ. We also postulate the existence of a radius  $r_b$  below which the amplitude of the meridional circulation becomes negligible. The existence of such a radius can be inferred based on the presence of the solar tachocline as deduced from helioseismology. In the absence of other forces, the combined effects of gyroscopic pumping, thermal wind balance, and radiative diffusion would induce a meridional circulation below the convection zone that would

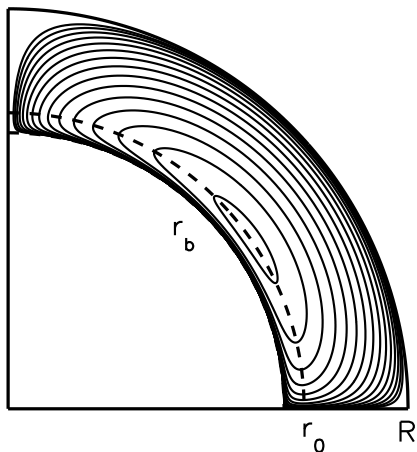


FIG. 1.— Schematic diagram illustrating  $r_0$  and  $r_b$  for an idealized single-cell meridional circulation profile. Both radii are indicated by dashed lines, although the latter is difficult to distinguish from the streamlines of the mass flux, indicated by solid lines. The northern hemisphere is shown and the sense of the circulation is counter-clockwise. The turnaround radius  $r_0$  marks a change in sign of the latitudinal flow while  $r_b$  marks the radius below which the circulation is negligible. The radius of the Sun is denoted by  $R$ . Thus, equatorward flow occurs for  $r_b < r < r_0$  and poleward flow for  $r_0 < r < R$ .

wipe out the radial shear in the tachocline, causing the latitudinal shear to spread downward on a time scale of several billion years (Spiegel & Zahn 1992). Helioseismic inversions indicate that this has not happened, suggesting the presence of some unknown torques that act to confine the tachocline (e.g. Miesch 2005). Thus, the thinness of the tachocline inferred from helioseismic rotation inversions suggests that the amplitude of the meridional circulation likely drops off rapidly below the base of the convection zone (Garaud & Arreguin 2009).

So, in light of eq. (1),  $r_0$  separates the the region of poleward flow and flux divergence ( $\mathcal{F} < 0$ ),  $r_0 \leq r \leq R$ , from the region of equatorward flow and flux convergence ( $\mathcal{F} > 0$ ),  $r_b \leq r \leq r_0$ . Equation (9) effectively assumes that the width of these layers is comparable, such that  $r_0 - r_b \approx R - r_0$ . In other words, this equation breaks down if the equatorward flow is confined to a much smaller region than the poleward flow, or vice versa. In this case the effective  $L_t = r_0 - r_b$  could become arbitrarily small, implying small values of  $\delta$  ( $\ll 1$ ). A similar caveat also holds for the multi-celled case  $N_c > 1$ .

The mechanical forcing required to establish an asymmetric meridional circulation profile such as that depicted in Figure 1 via gyroscopic pumping may or may not be convective in origin (*asymmetric* in the sense that  $r_0 - r_b \ll R - r_0$ ). A localized convergence of angular momentum flux could arise from the convective Reynolds stress as convective plumes are rapidly decelerated by the subadiabatic stratification near the base of the CZ. Alternatively, it could arise from whatever non-convective processes may be involved in tachocline confinement, such as large-scale Lorentz forces or Reynolds and Maxwell stresses induced by MHD instabilities (Spiegel & Zahn 1992; Gough & McIntyre 1998; Miesch 2005). Whatever its origin, the confinement mechanism would have to transport angular momentum poleward in order to prevent the radiative spreading of the tachocline. This would imply a convergence of angular momentum at mid

to high latitudes that would in turn induce a prograde torque and an equatorward flow by means of gyroscopic pumping. This may plausibly be confined to a thin boundary layer in the vicinity of the tachocline.

Regardless of how thin the region of equatorward flow may be, conservation of mass requires that there be a net poleward flow in the remainder of the CZ, implying a flux divergence. Might this also occur in a thin layer, such that  $\delta \ll 1$ ? If so, wouldn't equation (7) imply that  $V_c$  could be arbitrarily small? In other words, could weak convection maintain the observed mean flows in the solar interior by establishing a Reynolds stress that is nearly divergenceless in the bulk of the CZ, with narrow regions of divergence and convergence in the upper and lower boundary layers? In the remainder of this section we argue that the answer to this question is likely to be no. Although this scenario is in principle consistent with the physics of gyroscopic pumping, it can be largely ruled out by helioseismic measurements.

We begin with a direct estimate of  $\delta$  in the surface layers obtained from helioseismic determinations of the meridional flow. As noted in §1, local helioseismic inversions suggest that the radius at which the poleward surface flow reverses sign is no shallower than  $0.95R$ , so  $R - r_0 \gtrsim 0.05R$ . If we equate this with  $L_t$ , this provides a lower bound for  $\delta$  in the surface layers:

$$\delta \sim \sqrt{2}L_t/R \gtrsim 0.07 \quad (\text{surface layers}) \quad . \quad (10)$$

Thus, the factor of  $\delta^{1/2}$  in eq. (7) is likely to be no smaller than 0.26 in the surface layers.

We now consider the nonlocal nature of gyroscopic pumping, which provides a link between regions of Reynolds stress convergence and divergence even if they are spatially separated (MH11). Local forcing can in principle induce a global meridional flow that couples the two regions, even if they are localized in the upper and lower boundary layers. Furthermore, since isosurfaces of  $\mathcal{L}$  are approximately radial at high latitudes, a single circulation cell with poleward flow at the surface, downward flow near the poles, and equatorward flow at the base of the CZ could in principle be sustained even if the high-latitude Reynolds stress were divergenceless in the bulk of the CZ ( $\mathcal{F} \approx 0$ ).

However,  $\mathcal{F}$  cannot be zero in the bulk of the CZ at low latitudes. Mass conservation requires a radially outward meridional flow that must be balanced by the Reynolds stress. If it were not, the circulation would quickly homogenize  $\mathcal{L}$  at the equator, establishing an inward  $\Omega$  gradient ( $\Omega \propto r^{-2}$ ) on a crossing time scale  $\sim D/V_m$  (about 6 years for  $V_m \sim 1 \text{ m s}^{-1}$ ). Thus, the  $\Omega$  profile and the horizontal divergence of the meridional flow inferred from solar observations provide a robust diagnostic of the Reynolds stress at the equator. We now exploit this diagnostic to obtain alternative estimates for  $\delta$  and  $V_c$ .

Symmetry requires that the radial component of the flux divergence on the RHS of (2) vanish at the equator, so  $L_t$  must correspond to the latitudinal convergence of the angular momentum flux that sustains the radially outward  $V_m$ . Since the convergence of  $\mathcal{F}$  must span all latitudes where the flow is outward, we can estimate  $L_t$  from the outward mass flux  $\dot{M} = \rho V_m 2\pi r L_t$ . We have defined  $\dot{M}$  to be the outward mass flux in one hemisphere because in §3.2 we will equate it to the observed poleward

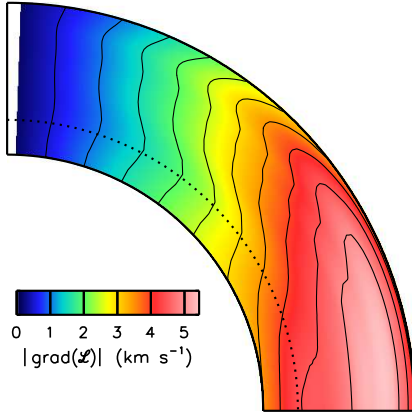


FIG. 2.— Shown is the magnitude of the specific angular momentum gradient  $|\nabla\mathcal{L}|$  inferred from helioseismic rotational inversions. For the corresponding profiles of  $\Omega$  and  $\mathcal{L}$  see Fig. 1 of MH11. These results are based on RLS inversions of GONG data from four non-overlapping intervals in 1996, provided by R. Howe (Howe et al. 2000; Schou et al. 2002). The dotted line indicates the base of the convection zone.

mass flux in the surface layers. Setting  $\lambda = r$  at the equator then gives us an alternate estimate for  $\delta$

$$\delta = \frac{L_t}{\lambda} = \frac{\dot{M}}{\rho V_m 2\pi r^2} \quad (V_m = |\langle v_r \rangle| \text{ at } 0^\circ \text{ lat}) \quad (11)$$

Substituting this expression into (7) yields

$$V_c \gtrsim \left( \frac{\dot{M} |\nabla\mathcal{L}|}{2\pi r^2 \rho} \right)^{1/2} \quad (V_m = |\langle v_r \rangle| \text{ at } 0^\circ \text{ lat}). \quad (12)$$

Note that the meridional flow only appears in Eq. (12) through the mass flux  $\dot{M}$ , which we can estimate from helioseismic inversions (§3.2). Since  $\mathcal{L}$  and  $\rho$  are also known from helioseismology and solar structure models, Eq. (12) provides a robust lower limit on the convective velocity near the equator that is independent of  $\delta$ . Given the observed uniformity of the solar irradiance (Rast et al. 2008), velocity amplitudes at higher latitudes are likely to be comparable.

In summary, Eq. (12) provides a reliable lower limit on the convective velocity amplitude at low latitudes based firmly in observable quantities. The estimate is most reliable at a radius of  $r \sim 0.95R$  (above which we know that the meridional flow is poleward) but it can be extended to lower radii if a single-celled profile ( $N_c = 1$ ) is assumed. Equation (10) is also robust, depending only on helioseismic inversions in the surface layers. Together with Eqs. (7) and (8) it provides a reliable, though somewhat conservative, limit on the convective velocities above  $0.95R$ .

Equation (9) can be used together with Eqs. (7) and (8) to provide estimates of  $V_c$  in the lower CZ at mid-latitudes. However, these estimates break down if there is a large difference in the filling factor between polar and equatorial flows. For example, if  $N_c = 1$  and if the return equatorward flow near the base of the CZ is confined to a very small region such that  $r_0 - r_b \ll R - r_0$ , then the effective  $\delta$  near the base of the CZ could be significantly smaller than the estimate given in Eq. (9). This would in turn reduce the lower limit on  $V_c$  near the base of the

CZ according to Eqs. (7) and (8).

In the next section (§3.2) we quantify our estimates by turning to photospheric observations and helioseismic inversions. However, before proceeding, we briefly address the possibility of multiple circulation cells in latitude.

In short, the analysis and conclusions of this paper are insensitive to the high-latitude structure of the meridional flow. Our focus is not on the mean flows themselves, but on using mean flow measurements as tools to probe the convection. Since helioseismic inversions of differential rotation and meridional flow are most reliable at low to mid latitudes, this is where we focus our attention. These indicate a single circulation cell near the surface up to latitudes of at least  $50\text{--}60^\circ$ . According to the gyroscopic pumping equation (1), the presence of one or more high-latitude counter-cells may signify a change in the sense and possibly the amplitude of the Reynolds stress, which may in turn signify a change in  $V_c$ . However, given the small latitudinal variation of the solar irradiance (Rast et al. 2008), it is more likely that a change in  $\mathcal{F}$  at high latitudes would be associated with a change in the efficiency factor  $\epsilon$ , the transport scale  $\delta$ , the angular momentum gradient  $|\nabla\mathcal{L}|$ , or other contributions to  $\mathcal{F}$  such as Maxwell stresses. These issues lie outside the scope of this paper.

### 3.2. Estimates Based on Helioseismic Inversions

In §3.1 we gave a conservative estimate of  $|\nabla\mathcal{L}|$  by considering only the uniform rotation component. A more precise estimate follows straightforwardly from helioseismic rotational inversions and is shown in Fig. 2. At mid-latitudes its magnitude is roughly  $3 \text{ km s}^{-1}$ , slightly larger than the value associated with the uniform rotation component,  $|\nabla\mathcal{L}_0| \sim 2V_\Omega \sim 2.7 \text{ km s}^{-1}$ . This is a consequence of the sense of the differential rotation, prograde at the equator and retrograde at the poles, which enhances the cylindrically outward  $\nabla\mathcal{L}$ . Thus, the simple lower limit expressed in (8) is still valid for the Sun when the differential rotation is taken into account. The same is true for any star with a solar-like differential rotation (equatorward  $\nabla\Omega$ ).

An estimate for  $V_m$  is harder to come by but we do have two pieces of reliable information from solar observations that we will exploit. First, the mean meridional flow at mid-latitudes is poleward on average near the surface for  $r \gtrsim 0.95R$ , with an amplitude of about  $10\text{--}20 \text{ m s}^{-1}$  (§1). Second, solar structure models provide a reliable measure of the density throughout the convection zone that is verified by helioseismic structure inversions to within a few percent (Christensen-Dalsgaard 2002). We now proceed to use these two foundations together with mass conservation to obtain a lower bound on  $V_m$ .

We begin by estimating the poleward mass flux near the surface at mid-latitudes

$$\dot{M} = 2\pi \int_{r_s}^R \langle \rho v_\theta \rangle r dr \equiv 2\pi \tilde{V}_\theta \int_{r_s}^R \rho r dr \quad , \quad (13)$$

where  $r_s = 0.95R$  and we will take  $\rho$  from Model S (see §3.1). In order to obtain a lower limit on  $V_m$ , and thus, the convective velocity  $V_c$ , we take the mass-weighted poleward flow near the surface to be  $\tilde{V}_\theta \sim 10 \text{ m s}^{-1}$ , which gives  $\dot{M} \sim 4.1 \times 10^{21} \text{ g s}^{-1}$ .

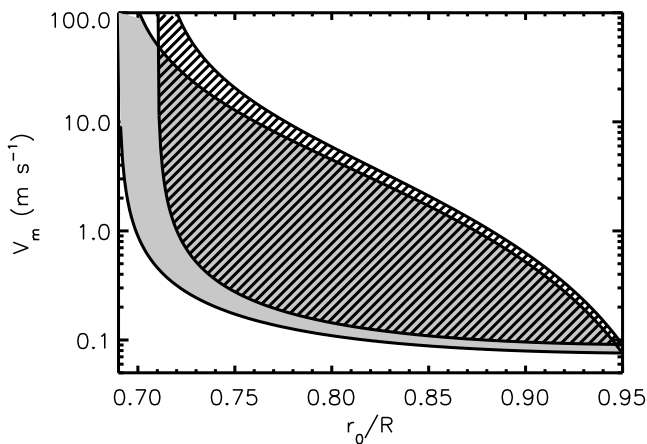


FIG. 3.— Magnitude of the deep meridional flow  $\tilde{V}_m$  as a function of the turnaround radius  $r_0/R$  estimated from Eq. (14) for  $r_b = 0.69R$  (grey shaded area) and  $r_b = 0.71$  (hatched area). Each area is bounded by the lower curve, given by  $\dot{M} = 4.1 \times 10^{21} \text{ g s}^{-1}$  and an upper curve where  $\dot{M}$  is given by Eq. (13) with  $r_s$  replaced by  $r_0$  and  $\tilde{V}_\theta = 10 \text{ m s}^{-1}$ .

We treat  $\dot{M}$  as a known quantity and estimate the average (density-weighted) deep return flow  $V_m$  based on mass conservation as

$$V_m \sim \dot{M} \left( 2\pi \int_{r_b}^{r_0} \rho r dr \right)^{-1}. \quad (14)$$

Here  $r_b$  is the radius below which the meridional flow is negligible and  $r_0$  is the turnaround radius where the mean flow shifts from poleward to equatorward (see Fig. 1 and the associated discussion in §3.1). Note that this does not preclude multiple cells in radius; regardless of the meridional flow profile, there must be a net equatorward flow below  $r_s$  to balance the poleward flow above  $r_s$ . Note also that some component of this return flow must necessarily cross  $\mathcal{L}$  contours (which are approximately cylindrical: see MH11), requiring a Reynolds stress to maintain it as expressed in Eq. (2).

Figure 3 shows estimates of  $V_m$  based on two different assumptions for the base of the main circulation cell,  $r_b$ . A robust lower limit for  $V_m$  is obtained by setting  $\dot{M}$  to be the value known for the near-surface flow above  $0.95R$ . An upper limit follows if we assume that the  $10 \text{ m s}^{-1}$  poleward flow persists for the entire region above the turnaround radius  $r > r_0$ . Then the deep flow  $V_m$  must be correspondingly stronger to balance the greater poleward mass flux. The actual meridional flow speed is likely to lie between these limits, as indicated in Fig. 3.

We are now able to obtain quantitative limits on  $V_c$  based on the expressions derived in §3.1. Taking  $|\nabla \mathcal{L}| \sim 3 \text{ km s}^{-1}$  at mid latitudes from Fig. 2 and  $\delta$  from Eq. (9) and substitute them into Eq. (7) gives

$$V_c \gtrsim 27 \text{ m s}^{-1} N_c^{-1/2} \left( \frac{V_m}{1 \text{ m s}^{-1}} \right)^{1/2}. \quad (15)$$

Thus, if the latitudinal flow speed  $V_m$  lies somewhere between  $0.1$ – $10 \text{ m s}^{-1}$  as suggested by Figure 3, then the lower limit for  $V_c$  in Eq. (15) lies somewhere between  $8.6$ – $86 \text{ m s}^{-1}$ .

The higher end of the range,  $\sim 86 \text{ m s}^{-1}$ , will apply near the surface ( $r \gtrsim 0.95R$ ) where the meridional flow speed is known to be  $10$ – $15 \text{ m s}^{-1}$ . The lower estimate of  $8.6 \text{ m s}^{-1}$  only applies if the meridional flow speed is as slow as  $0.1 \text{ m s}^{-1}$  near the base of the CZ, if it penetrates deeper than  $0.69R$ , or if the circulation profile is multicelled ( $N_c > 1$ ). Lower values of  $V_c$  are also possible if the meridional flow near the base of the convection zone is confined to a narrow layer in radius as described in §3.1. Near the top of the CZ, Eqs. (10) and (7) give a more reliable but more conservative estimate of  $V_c \gtrsim 45 \text{ m s}^{-1}$ .

Recall that these estimates are based on the latitudinal flow speed at mid latitudes. By contrast, the estimate given in Eq. (12) is based on the radial flow at the equator. Thus, for this estimate, we use the larger equatorial value of  $|\nabla \mathcal{L}| \sim 5 \text{ km s}^{-1}$  indicated by Fig. 2. We also equate the upward mass flux at the equator with the poleward mass flux above  $r \sim 0.95R$  inferred from local helioseismology. As noted above, this gives a value of  $\dot{M} = 4.1 \times 10^{21} \text{ g s}^{-1}$ . Substituting these values into Eq. (12) yields

$$V_c \gtrsim 30 \text{ m s}^{-1} \left[ \frac{\rho}{0.008 \text{ g cm}^{-3}} \right]^{-1/2} \left[ \frac{r}{0.95R} \right]^{-1} \quad (16)$$

As noted in §3.1, this estimate is most reliable at  $r \sim 0.95R$  above which the meridional flow is known to be poleward so we have a reliable estimate for  $\dot{M}$ . The value of  $\rho = 0.008 \text{ g cm}^{-3}$  used in Eq. (16) is based on Model S at  $r \sim 0.95R$ . If we assume this outward mass flux extends down to the lower CZ, then Eq. (16) implies  $V_c \gtrsim 9 \text{ m s}^{-1}$  at  $r \sim 0.75R$  (where  $\rho \sim 0.14 \text{ g cm}^{-3}$ ).

Combining these separate estimates, we conclude that the amplitude of convective velocities must be at least  $30 \text{ m s}^{-1}$  in the upper CZ ( $r \sim 0.95R$ ) and at least  $8 \text{ m s}^{-1}$  in the lower CZ ( $r \sim 0.75R$ ). These of course are lower limits so larger amplitudes are entirely possible and even likely.

#### 4. DISCUSSION

##### 4.1. Length Scales and Implications for Detectability

The lower limits obtained for convective velocities in §3 make no reference to the characteristic length scale at which the convective motions occur. In this section we address this issue and consider its implications for the detectability of deep convection by means of local helioseismology.

Some insight into the characteristic length scale  $L_c$  for deep convection can be obtained by considering the Rossby number  $R_o = V_c/(2\Omega L_c)$ . As is well known,  $R_o$  quantifies the amplitude of advective momentum transport in a rotating reference frame relative to the Coriolis force; small values  $R_o \lesssim 1$  imply strong rotational influence and large values weak.

Numerical simulations of convection exhibit a profound change in the nature of convective angular momentum transport as the Rossby number varies across unity. When the rotational influence is weak  $R_o > 1$ , convective flows tend to conserve their angular momentum locally, producing anti-solar differential rotation profiles in which the angular velocity increases toward the rotation axis, implying  $\partial\Omega/\partial\theta < 0$  in the NH



(Gilman 1977; Gilman & Foukal 1979; Hathaway 1982; DeRosa et al. 2002; Aurnou et al. 2007; Augustson et al. 2011; Featherstone et al. 2012). As the rotational influence becomes stronger, the preferred convective modes tend to align with the rotation axis, and the resulting velocity correlations induce an equatorward angular momentum transport by means of the convective Reynolds stress (Busse 2002; Miesch & Toomre 2009). This generally promotes solar-like angular velocity profiles in which the angular velocity gradient is equatorward ( $\partial\Omega/\partial\theta > 0$  in the northern hemisphere). It is currently an open question precisely where this transition lies but simulations suggest that it occurs for values of  $R_o$  somewhat less than unity, perhaps around  $0.6 \pm 0.3$  (Featherstone et al. 2012).

Although this insight is based on convection simulations (which, like any model, have limitations), there is good reason to suspect that it still applies in the extreme parameter regime of the solar interior. Consider a radial downflow convective plume that is accelerated in the upper thermal boundary layer of the Sun, near the photosphere. The Coriolis force operating on this plume will tend to deflect it in a prograde direction with a characteristic time scale of  $\tau \sim (2\Omega_0)^{-1}$  and a radius of curvature  $r_c = V_c/(2\Omega_0)$ . If the vertical coherence of the plume in the absence of rotation is  $L_c$  then we obtain  $r_c/L_c = R_o$ .

To appreciate the significance of this, consider the equatorial plane ( $\sin\theta = 1$ ) and set  $L_c$  to be the depth of the convection zone. If  $R_o \gg 1$ , the plume is deflected only slightly in a prograde direction before it reaches the base of the convection zone. This will induce a negative  $\langle v'_r v'_\phi \rangle$  correlation, producing cylindrically inward angular momentum transport and an anti-solar differential rotation profile. However, if  $r_c$  is less than the depth of the CZ, then our idealized, ballistic plume will never make it to the bottom. The vertical dominance of the flow will be broken and the nature of the Reynolds stress will be profoundly altered. This argument can be readily generalized to any intrinsic vertical coherence length  $L_c$  and any latitude, with an effective radius of curvature of  $r_c/\sin\theta$ .

More generally, it is reasonable to argue that only motions with  $R_o < 1$  will possess a rotational influence strong enough to establish the solar differential rotation (for  $r \lesssim 0.95R$ ). The corresponding length scale  $L_c \sim V_c/(2\Omega_0 R_o)$  can be expressed in terms of the spherical harmonic degree  $\ell \sim 2\pi r/L_c$ , as follows;

$$\ell \sim \frac{4\pi r \Omega_0}{V_c} R_o \lesssim 750 R_o \left[ \frac{V_c}{30 \text{ m s}^{-1}} \right]^{-1}. \quad (17)$$

For the numerical estimate we have used  $\Omega_0 = 2.7 \times 10^{-6}$  and  $r = 0.95R$ . Note that  $\ell = 750$  corresponds to a physical length scale of 5.5 Mm.

Thus, setting  $R_o < 1$  in Eq. (17) suggests that the convective motions responsible for maintaining the solar differential rotation and meridional circulation must occur at spherical harmonic degree no greater than 750, implying a length scale no less than 5.5 Mm.

Note that the values used to obtain the numerical estimate in Eq. (17), namely  $r = 0.95R$  and  $V_c \gtrsim 30 \text{ m s}^{-1}$  correspond to the base of the near-surface shear layer

where the transition from large to small Rossby number apparently occurs (MH11). Note also that these values are almost certainly a conservative estimate. If the transitional Rossby number is closer to 0.5, the convective velocity scale is closer to  $50 \text{ m s}^{-1}$  and the efficiency factor in Eq. (6) is closer to 0.5, then the lower limit in Eq. (17) assumes plausible values of  $\ell \sim 160$  and  $L_c \sim 25 \text{ Mm}$ . One might also argue that convective motions below  $0.95R$  are likely to occupy scales no smaller than supergranules, which would imply  $\ell \lesssim 130$  and  $L_c \gtrsim 30 \text{ Mm}$ .

These latter values are remarkably close to the the density and pressure scale heights,  $H_\rho$  and  $H_P$ , which provide an independent estimate for  $L_c$  by virtue of mixing length theory. According to Model S,  $H_\rho \sim 20 \text{ Mm}$  and  $H_P \sim 12 \text{ Mm}$  at  $r = 0.95R$ , increasing steadily to 90 and 57 Mm respectively at the CZ base. Interestingly, if we assume that the length scale of convective motions at  $r = 0.95R$  is equal to the density scale height,  $L_c \sim 20 \text{ Mm}$ , then this implies that the transition from strong to weak rotational influence that marks the base of the NSSL occurs at a Rossby number of about 0.28.

More generally, mixing-length theory predicts that  $L_c$  should increase with decreasing  $r$ , becoming larger near the base of the CZ. A naive application of Eq. (17) suggests the opposite; inserting our estimate of  $V_c \gtrsim 8 \text{ m s}^{-1}$  in the lower CZ would push the limit toward higher  $\ell$ . However, this is a misapplication of Eq. (17). Convection simulations and mixing length theory suggest that the Rossby number should decrease toward the base of the CZ more rapidly than  $V_c$ , implying an increase in  $L_c$ .

As mentioned in §1, recent work by Hanasoge et al. (2010, 2012) based on local helioseismic inversions suggests that the spectral amplitude of convective motions may be no more than  $1 \text{ m s}^{-1}$  on scales  $\ell \lesssim 60$  at a radius of  $r \sim 0.92\text{--}0.95 R$ . Smaller horizontal scales (higher  $\ell$ ) lie beyond their detection limits at that depth. This is difficult to reconcile with our lower limit of  $30 \text{ m s}^{-1}$  but may be possible if deep solar convection occupies multiple disparate scales, with broad, weak upflows surrounding very narrow downflows. This may well yield small spectral amplitudes for global-scale modes ( $\ell < 60$ ) while local velocities in downflows might be much higher. However, this still poses significant challenges to our current paradigm for how solar mean flows are maintained.

In summary, the lower limits on convective velocities obtained in §3 based on the maintenance of mean flows and the upper limits obtained by Hanasoge et al. (2010) based on local helioseismic inversions are both consistent with the idea that the characteristic length scale of convective motions is comparable to the local scale heights  $H_\rho$  and  $H_P$ . This yields Rossby numbers less than unity in the deep convection zone where mean flows are established and Rossby numbers greater than unity in the near-surface shear layer, as suggested by solar observations (MH11).

Finally, we note that the estimated length scales discussed here bode well for the future of global solar convection simulations. In order to adequately resolve a structure of size  $L_c$ , a simulation should have a resolution of at least  $\sim 0.1L_c$ . Thus, if  $R_o \sim 1$ , Eq. (17) suggests that a resolution as high as  $\ell \sim 7500$  (grid spacing  $\delta \sim 0.65 \text{ Mm}$ ) could be required to capture the relevant dynamics. This is beyond the current capabilities of global



models but recall that this is a conservative limit. For plausible values in the mid CZ of  $R_o \sim 0.2$ ,  $V_c \sim 50$  m s $^{-1}$  and  $\epsilon \sim 0.5$ , Eq. (17) implies  $\ell \lesssim 64$  ( $L_c \gtrsim 65$  Mm). Thus, a resolution extending to  $\ell \sim 640$  should be sufficient to capture the dominant physical scales. This is achievable now with current global simulations (Miesch et al. 2008).

This is not to say that current simulations necessarily capture all of the relevant dynamics. But, to put it colloquially, they're beginning to approach the right ballpark. This suggests that we may be near a threshold in the sense that moderate increases in resolution, together with improved modeling of the surface boundary layer and the overshoot region, could yield significant advances in our understanding of solar convection and the mean flows it establishes. This may be achieved both through the availability of increasingly powerful computing resources and through improved numerical algorithms that achieve higher parallel efficiency.

#### 4.2. Consistency with Convection Models

We emphasize again that the limits on the convective velocities deduced in §3.1 and §3.2 do not depend on any theoretical or numerical model other than the basic MHD equations and the dynamical balance expressed by Eq. (2). Thus, it is of interest to ask whether theoretical and numerical models of convection are indeed consistent with these limits.

The short answer is yes; models of solar convection based on several disparate physical perspectives and modeling approaches are uniformly consistent with the ideas proposed in this paper. This is demonstrated in Figure 4.

Shown in the Figure are results from global convection simulations based on the ASH code (black line, see Weber et al. 2011 for more information about this particular simulation), surface convection simulations based on the MURAM code (red line, see Vögler et al. 2005 and Rempel et al. 2009 for a description of the model and Rempel 2011 for more details on this series of simulations), and a hybrid model that combines surface convection simulations (from the STAGGER code) with a deep extrapolation based on mixing-length theory (blue line, see Trampedach & Stein 2011 for more information). Note that both surface convection simulations presented here correspond to the quiet sun, with no active regions or flux emergence.

Superposed on the various curves are horizontal lines representing the theoretical lower limit for  $V_c$  obtained from Eq. (15) with  $V_m = 1.0, 10$ , and  $25$  m s $^{-1}$ . All curves lie above the first limit, implying that the convective motions are at least in principle strong enough to sustain a solar-like differential rotation with a meridional flow of order  $1$  m s $^{-1}$  or less in the deep CZ. However, they are only strong enough to sustain a meridional flow speed  $\gtrsim 25$  m s $^{-1}$  in the upper half of the CZ. So, the convective amplitudes are consistent with mean flows inferred from solar observations and they confirm the expectation from mass conservation that the flow speed of the deep equatorward return flow is likely to be less than the poleward surface value of  $10$ – $20$  m s $^{-1}$ . Furthermore, all curves satisfy the limits obtained from Eq. (16) of  $V_c \gtrsim 30$  m s $^{-1}$  and  $V_c \gtrsim 9$  m s $^{-1}$  in the upper and lower CZ respectively and all curves satisfy the limit of

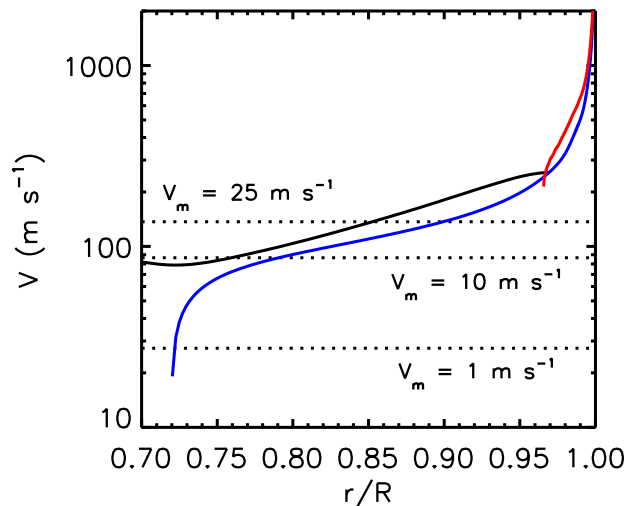


FIG. 4.— Comparison of theoretical lower limits for the convection amplitude (dotted lines) with numerical and theoretical models of convection (solid lines). The three dotted lines are obtained from Eq. (15) with  $V_m = 1.0, 10$  and  $25$  m s $^{-1}$  as indicated. The black line is obtained from a global convection simulation with the ASH code (described in Weber et al. 2011) and the brown line is from a simulation of surface convection done with the MURAM code (Vögler et al. 2005; Rempel et al. 2009). The blue line is from a composite model combining surface convection simulations with the STAGGER code ( $r > 0.97R$ ) with a mixing length model ( $r < 0.97R$ ), the latter calibrated to give the same entropy jump as the simulation and scaled for continuity (Trampedach & Stein 2011).

$V_c \gtrsim 45$  m s $^{-1}$  for  $r \gtrsim 0.95R$  obtained from eqs. (7) and (10).

Further confirmation of the consistency of these models comes from mean-field models of the solar differential rotation and meridional circulation by Rempel (2005, 2006). Here the convective amplitudes are essentially prescribed *a priori* by means of the imposed Reynolds stress, modeled as a turbulent diffusion plus a  $\Lambda$ -effect. This is in contrast to the convection simulations shown in Figure 4 where  $V_c$  is a product of the simulation. However, these mean-field models can be calibrated to produce solar-like mean flows so estimates of  $V_c$  can be obtained by selecting the optimal transport coefficients. Here we are interested in particular in the  $\Lambda$ -effect, which is the non-diffusive component of the Reynolds stress tensor responsible for maintaining the differential rotation and, ultimately, the meridional circulation by means of gyroscopic pumping (§2.1).

In Rempel's models, the amplitude of the  $\Lambda$ -effect is given by  $\Lambda_0 \nu_t \Omega_0$  where  $\Lambda_0$  is a non-dimensional coefficient of order unity and  $\nu_t$  is the turbulent viscosity. Relating this to the convective velocity as in Eq. (6) yields  $V_c \gtrsim (\Lambda_0 \nu_t \Omega_0)^{1/2}$  for  $\epsilon \leq 1$ . Solar-like mean flows are generally obtained with  $\Lambda_0 \sim 0.8$  and  $\nu_t \sim 3$ – $5 \times 10^{12}$  cm $^2$  s $^{-1}$  in the bulk of the CZ. Near the base of the CZ,  $\nu_t$  drops sharply by more than an order of magnitude.

The value of  $\nu_t \sim 3$ – $5 \times 10^{12}$  cm $^2$  s $^{-1}$  in the upper CZ implies  $V_c \gtrsim 25$ – $35$  m s $^{-1}$ . This is comparable to our estimate of  $V_c \gtrsim 30$  m s $^{-1}$  based on Eq. (12). However, this lower limit lies below the limit of  $V_c \gtrsim 86$  m s $^{-1}$  in the upper CZ based on Eq. (15) and  $V_c \gtrsim 45$  m s $^{-1}$  based

on Eqs. (7) and (10). This implies that the effective value of  $\delta$  in the upper CZ is somewhat smaller than that given by Eqs. (9) and (10). Since  $\nu_t$  is nearly constant in the upper CZ, this smaller value of  $\delta$  can be attributed to the density gradient, which factors into the Reynolds stress as indicated in Eq. (2). Similarly, a strong convergence of the angular momentum flux ( $\delta \ll 1$ ) near the base of the CZ (associated with the sharp drop in  $\nu_t$ ) sustains an equatorward flow of a few  $\text{m s}^{-1}$  despite the low value of  $\nu_t$ .

The value of  $\nu_t$  used by Rempel was deliberately chosen to be relatively small in order to make it more compatible with the small value of the turbulent magnetic diffusivity  $\eta_t \sim 10^{11} \text{ cm}^2 \text{ s}^{-1}$  in the mid CZ, needed for the operation of the advection-dominated flux-transport dynamo (§4.3). In many mean-field theories such as that of Kitchatinov & Rüdiger (2005),  $\nu_t$  is significantly larger, often exceeding  $10^{13} \text{ cm}^2 \text{ s}^{-1}$  as predicted by mixing-length theory.

The consistency among these disparate models is remarkable. The surface convection simulations (blue and red curves in Fig. 4) make good contact with photospheric observations of convective amplitudes but they do not address mean flows; differential rotation and meridional circulation lie outside the scope of the models. Meanwhile, the global convection simulations self-consistently produce a solar-like differential rotation and the convective velocity amplitudes roughly match the surface convection simulations (to within about 20%) in their small region of overlap near  $r \sim 0.97R$ . Furthermore, the global (ASH) simulation satisfies the constraint in Eq. (7) with  $\delta \sim 0.25$  and meridional flow speeds are consistent with Figure 3, with values of a few  $\text{m s}^{-1}$  near the base of the CZ and  $\sim 10\text{--}20 \text{ m s}^{-1}$  near the surface. The mean-field models by Rempel (2005, 2006) produce solar-like mean flows with Reynolds stress amplitudes somewhat lower than suggested by the convective models but they are consistent with an efficiency factor of  $\epsilon < 1$ . Furthermore, they are still consistent with the velocity estimates put forth in §3 when one takes into account the relatively sharp gradients in the imposed angular momentum flux (small  $\delta$ ), particularly at the base of the CZ.

We also note that our lower limit for  $V_c$  of  $8 \text{ m s}^{-1}$  at the base of the CZ is consistent with the upper limit of  $V_c < 50 \text{ m s}^{-1}$  obtained by Isik & Holzwarth (2009) based on numerical models of the interaction between thin flux tubes and convective flows. Larger convection amplitudes disrupt the flux storage, promoting buoyancy instabilities on time scales shorter than the dynamo amplification time of a few years.

#### 4.3. Implications for Flux-Transport Dynamo Models

Arguably one of the most successful (and certainly one of the most popular) current paradigms for modeling the origin of the solar activity cycle is the flux-transport dynamo. For recent reviews see Dikpati & Gilman (2009) and Charbonneau (2010) and for further details see Wang et al. (1991); Choudhuri et al. (1995); Dikpati & Charbonneau (1999); Dikpati & Gilman (2001, 2006); Küker et al. (2001); Nandy & Choudhuri (2001); Bonanno et al. (2002); Rempel (2006); Jouve & Brun (2007); Jiang et al. (2007); Yeates et al.

(2008); Guerrero et al. (2009); Munoz-Jaramillo et al. (2009, 2011); Hotta & Yokoyama (2010), and many more.

Flux-transport (FT) dynamo models are mean-field models that solve the axisymmetric MHD induction equation, typically in the kinematic limit. Like other mean-field models, they involve specified prescriptions for magnetic field generation and transport by non-axisymmetric motions such as convection and flux emergence that lie outside the scope of the model. Their defining characteristic that sets them apart from other mean-field models is that the mean meridional circulation plays an essential role in transporting magnetic flux and in thereby regulating the cycle period.

Of particular importance is the direction and speed of the meridional flow near the base of the convection zone. There, an equatorward flow with a speed of  $2\text{--}4 \text{ m s}^{-1}$  provides a robust mechanism for producing solar-like butterfly diagrams, whereby the mean toroidal field (taken as a proxy for sunspots) migrates toward the equator on a time scale of about 11 years.

Most FT models are also Babcock-Leighton models in which the emergence and subsequent dispersal of active region flux in the photosphere acts as a source for mean poloidal field (e.g. Charbonneau 2010). If this is the principal source of poloidal flux and if the mean toroidal field is generated near the base of the convection zone as in most models, then the dynamo requires a transport mechanism in order to operate. The two principal transport mechanisms considered in the literature are the meridional circulation and turbulent transport, the latter typically represented as a turbulent diffusion or magnetic pumping. Thus, Babcock-Leighton FT models may be further classified as advection-dominated or diffusion-dominated depending on which of these transport mechanisms plays a larger role (Yeates et al. 2008; Dikpati & Gilman 2009).

In short, the meridional circulation in advection-dominated FT dynamo models serves two roles. First, it regulates the cycle period through the equatorward transport of toroidal flux near the base of the CZ and second, it couples the spatially separated source regions for mean poloidal and toroidal flux. These two roles are distinct but they are not independent. For example, if the transport mechanism coupling poloidal and toroidal sources is too efficient, it can “short-circuit” the dynamo, reducing the cycle period by decreasing the effective path length at the base of the CZ over which the equatorward advection of toroidal flux operates.

The advection-dominated regime generally works well in the sense that it compares well with solar observations. Imposing a single-celled meridional flow in radius ( $N_c = 1$ ) with a poleward flow speed of  $10\text{--}20 \text{ m s}^{-1}$  near the surface as indicated by observations (§1) and an equatorward return flow of  $2\text{--}4 \text{ m s}^{-1}$  near the base of the convection zone (consistent with Fig. 3) generally produces solar-like magnetic cycles with a duration of about 11 years when used in conjunction with a solar-like differential rotation profile and a Babcock-Leighton source. More subtle issues such as dynamo parity, saturation, and cycle modulation have generally been handled through minor variations on this basic paradigm. For example, dipolar parity can be promoted

by an additional source of poloidal flux deeper in the CZ (Dikpati & Gilman 2001) or by enhanced turbulent diffusion in the surface layers (Hotta & Yokoyama 2010).

Although their empirical success and simplicity is rather compelling, the principle problem with FT dynamo models has always been the theoretical justification of the advection-dominated regime. In order for the meridional circulation to dominate the flux transport, convective transport must be relatively inefficient. Advection-dominated FT models typically model the latter as a turbulent diffusion and set the amplitude of the turbulent diffusivity  $\eta_t$  in the mid convection zone to be  $\sim 10^{11} \text{ cm}^2 \text{ s}^{-2}$  or less. This is at least two orders of magnitude smaller than estimates of  $\eta_t$  based on mixing-length theory and convection simulations; see Munoz-Jaramillo et al. (2011) for a more detailed discussion of the problem.

Our estimates of the convective velocity and length scales in §3 provide a measure of the convective transport that is independent of mixing length theory and convection simulations. Moreover, these estimates are directly linked to the amplitude and profile of the differential rotation and meridional circulation, which are essential ingredients in all FT dynamo models. Thus, to explore the implications of these estimates, we can take the actual mean flow profiles used in FT models as a starting point and then ask how strong the convective motions must be in order to maintain these flows.

The essence of the problem can be appreciated merely from equation (8). This suggests that the convective velocity must be of order the geometric mean between the rotational velocity and the meridional flow velocity, provided that the transport scale  $\delta$  is not inordinately small. As noted there, this implies  $V_c \gtrsim 47\text{--}106 \text{ m s}^{-1}$  for the meridional flow speeds of  $2\text{--}10 \text{ m s}^{-1}$  typically used in FT dynamo models. If we then assume that the size scale of the convection  $L_c$  is of order the density scale height of 60 Mm in the mid CZ, we obtain  $\eta_t \sim V_c L_c / 3 \sim 4 \times 10^{11} \text{--} 2 \times 10^{12} \text{ cm}^2 \text{ s}^{-1}$ . This is significantly higher than the values used in the lower CZ for many FT dynamo models. In what follows we provide a more detailed exposition of this result and its implications.

Thus, we begin with a standard FT dynamo model with a single-celled profile ( $N_c = 1$ ) and a solar-like differential rotation. If the turnaround radius  $r_0$  is near the middle of the CZ, then  $\delta$  is given by Eq. (9) and a lower limit on  $V_c$  is given by Eq. (15). Setting  $V_m \sim 2 \text{ m s}^{-1}$  near the base of the CZ implies  $V_c \gtrsim 38 \text{ m s}^{-1}$ . In the upper CZ we can set  $V_m \sim 10 \text{ m s}^{-1}$  which implies  $V_c \gtrsim 86 \text{ m s}^{-1}$ .

By combining these estimates of the velocity scale with the limits on the length scale  $L_c$  discussed in §4.1, we can obtain an estimate of the turbulent magnetic diffusivity  $\eta_t \sim V_c L_c / 3$ . Taking the very conservative limit of  $L_c \gtrsim 5.5 \text{ Mm}$  gives  $\eta_t \gtrsim 7 \times 10^{11} \text{ cm}^2 \text{ s}^{-1}$  near the bottom of the CZ and  $\eta_t \gtrsim 10^{12} \text{ cm}^2 \text{ s}^{-1}$  near the top. Although this is somewhat smaller than estimates based on mixing-length theory ( $\sim 10^{13}$ , see Munoz-Jaramillo et al. 2011), it is still nearly an order of magnitude larger than the values typically used in advection-dominated FT dynamo models. Using an estimate for  $L_c$  based on density or pressure scale heights increases  $\eta_t$  by nearly another order of magnitude (§4.1).

As noted in §3.1, these limits can be avoided if there is a strong convergence of the angular momentum flux near the base of the CZ which would effectively confine the equatorward return flow to a thin layer (this applies to the return flow of several  $\text{m s}^{-1}$  required for the operation of the FT dynamo; weaker equatorward flows may exist outside of this layer). In particular, the lower limit on  $V_c$  in Eq. (7) scales as  $L_t^{1/2}$  where  $L_t$  is the width of this layer. Reducing  $V_c$  enough to yield an  $\eta_t$  of  $10^{11} \text{ cm}^2 \text{ s}^{-1}$  would require that the equatorward return flow be confined to a layer no wider than

$$L_t \sim \frac{r_m V_c^2}{\sqrt{2} V_m |\nabla \mathcal{L}|} \sim 1.7 \text{ Mm} \sim 2 \times 10^{-3} R \quad (18)$$

Here we have used Eq. (7) with  $V_c = 3\eta_t/L_c$ ,  $\eta_t = 10^{11} \text{ cm}^2 \text{ s}^{-1}$ ,  $L_c = 5.5 \text{ Mm}$ ,  $V_m \sim 2 \text{ m s}^{-1}$ ,  $|\nabla \mathcal{L}| \sim 3 \text{ km s}^{-1}$ ,  $\delta \sim \sqrt{2} L_t / r_m$  and  $r_m = 0.7R$ . Larger values of  $L_c$  or  $V_m$  would imply even stronger gradients (smaller  $L_t$ ). Furthermore, since  $V_c^2$  scales as  $\epsilon^{-1}$  [see Eq. (7)], a value of  $\epsilon \sim 0.2$  as suggested by convection models (§3.1) would reduce the estimate of  $L_t$  in Eq. (18) by a factor of five, to 340 km. No current FT models employ such an extremely asymmetric meridional circulation profile and it is questionable whether efficient equatorward transport of strong toroidal flux concentrations could even occur in such a thin layer.

Even if such a thin layer were to exist near the base of the CZ,  $V_c$  and  $\eta$  would still have to be large enough in the upper CZ to satisfy Eqs. (10) [with Eq. (7)] and (16). These suggest that  $V_c$  must be at least  $30 \text{ m s}^{-1}$  at  $r \sim 0.95$ , independent of the deeper structure and amplitude of the meridional flow. If  $L_c \gtrsim 5.5 \text{ Mm}$  then this suggests  $\eta_t$  should be at least  $5.5 \times 10^{11} \text{ cm}^2 \text{ s}^{-1}$  in the upper CZ for any model with solar-like mean flows. This is in fact satisfied by many current FT models, but again, this is a conservative estimate. If  $L_c \gtrsim 30 \text{ Mm}$  and  $\epsilon \sim 0.2$ , this limit becomes much more stringent at  $\eta_t \gtrsim 6.7 \times 10^{12} \text{ cm}^2 \text{ s}^{-1}$ . In the lower CZ, for  $N_c = 1$ , Eq. (16) suggests  $\eta_t \gtrsim 1.6 \times 10^{11} \text{ cm}^2 \text{ s}^{-1}$  for  $L_c \gtrsim 5.5 \text{ Mm}$  and  $\epsilon \sim 1$  or  $\eta_t \gtrsim 2 \times 10^{12} \text{ cm}^2 \text{ s}^{-1}$  for  $L_c \gtrsim 30 \text{ Mm}$  and  $\epsilon \sim 0.2$ . Multiple cells in radius ( $N_c > 1$ ) could in principle help mitigate these limits on  $V_c$ ,  $\eta$ , and  $L_t$  but they are known to have an adverse effect on the operation of FT dynamos (Jouve & Brun 2007).

Thus, we conclude that current advection-dominated FT dynamo models are not strictly self-consistent. In particular, the amplitude of turbulent transport they typically assume is not commensurate with the mean flows they employ. Again, this has been argued before based on mixing-length theory and convection simulations but here we demonstrate more generally that it is a direct consequence of Eq. (2).

A potential way out of this dilemma is by moving to the diffusion-dominated regime. This would entail using values of  $\eta_t \gtrsim 10^{12} \text{ cm}^2 \text{ s}^{-1}$  throughout most of the convection zone. Such models have indeed had some success in modeling the solar cycle, and may actually do better in certain respects than advection-dominated models. Examples include reproducing the observed cycle amplitude-period relationship and triggering grand minima through variations in the meridional flow (Jiang et al. 2007; Yeates et al. 2008; Karak 2010).

However, it can be a challenge for diffusion-dominated FT models (or any model in which the transport by turbulent diffusion or magnetic pumping is very efficient) to achieve cycle periods as long as 11 years. As noted above, efficient turbulent transport in a Babcock-Leighton dynamo tends to short-circuit the region over which the dynamo operates and to thus decrease the cycle period. This is sometimes avoided by allowing the meridional circulation to extend well below the convection zone. However, if the turbulent diffusivity there is low, then these models may suffer from the same problem described here (namely that the local amplitude of  $\eta_t$  is incommensurate with the local amplitude of the meridional flow). Alternatively, one could place the turnover radius  $r_0$  higher up in the CZ to achieve a slower meridional flow in the lower CZ and thus a longer period (see Fig. 3). Still, the downward turbulent transport cannot be so efficient that it suppresses the poleward migration of residual flux from active regions that is seen in photospheric observations.

Alternatively, it has been argued that the quenching of turbulent transport by Lorentz force feedbacks may be able to salvage the advection-dominated regime (Guerrero et al. 2009; Munoz-Jaramillo et al. 2011). However, it remains to be seen whether or not this is viable. Quenching would be most effective for strong toroidal fields near the base of the CZ as opposed to the relatively weak poloidal fields whose turbulent transport across the CZ could potentially short-circuit the advection by the meridional flow. In other words, quenching is more likely to regulate the first role noted above for the meridional circulation in FT dynamos (equatorward advection of toroidal flux) as opposed to the second (coupling of poloidal and toroidal sources), and it is the second which generally defines the advection-dominated regime.

Furthermore, the arguments presented here demonstrate that a significant reduction in  $V_c$  by Lorentz force feedbacks as captured by quenching mechanisms would have substantial consequences for the mean flows. For example, if we treat  $V_\Omega$  as fixed, Eq. (8) indicates that a reduction in  $V_c$  by an order of magnitude may be accompanied by a reduction of the meridional flow speed  $V_m$  by two orders of magnitude (unless the efficiency factor  $\epsilon$  increases). This follows from the concept of gyroscopic pumping discussed in §2.1, provided that the nature of the Lorentz forces is solely to suppress convection. However, if the Lorentz force exerts its own mean torques, which is likely, then this should be included in the right-hand-side of Eq. (2), with corresponding modifications to Eqs. (7) and (8). The time dependence should also be taken into account, potentially mitigating limits on  $\eta_t$  for a given meridional flow speed. Even so, a self-consistent treatment of diffusivity quenching that takes into account its dynamical effect on the maintenance of mean flows could dramatically alter the operation of a FT dynamo by substantially modifying the meridional circulation and, to a lesser extent, the differential rotation.

A related possibility is that turbulent transport at very high magnetic Reynolds numbers may simply be less efficient than suggested by crude, kinematic representations based on the concept of turbulent diffusion. Nonlinear processes such as the dynamical alignment of fields and flows that contribute to dynamo saturation may also sup-

press turbulent transport in a way that is more subtle than a quenched local diffusion coefficient. This might require more sophisticated mean-field and/or MHD convection models to properly capture. Still another possibility, of course, is that the solar dynamo does not follow the canonical Babcock-Leighton/Flux-Transport paradigm.

## 5. SUMMARY

In this paper we estimate the amplitude and scale of the convective motions responsible for maintaining the solar differential rotation and meridional circulation. This estimate is based only on the observed properties of the mean flows in the Sun together with three fundamental physical premises grounded in the MHD equations.

The first and most important of these three premises is represented by Eq. (2). This tells us that, in order to achieve a statistically steady state, the angular momentum transport by the convective Reynolds stress must balance the advection of angular momentum by the meridional flow. This provides a direct link between the amplitude of mean flows and the amplitude of convective motions such that observations of the former can set constraints on the latter. Note that this dynamical balance is to be understood in a time-averaged sense, filtering out solar cycle variations of meridional and zonal flows.

The second physical premise we rely on is that of mass conservation [Eq. (1) in the Appendix]. This allows us to estimate the net equatorward flow speed in the deep CZ based on observations of the poleward flow near the surface as shown in Fig. 3. This result in turn allows us to extend the diagnostic power of our first premise to the deep convection zone where mean flows are established.

The third premise is that of thermal wind balance, Eq. (5). Although this is not used directly in our estimates for the convective velocity amplitude  $V_c$ , it helps to justify the concept of gyroscopic pumping discussed in §2.1. In particular, when coupled with helioseismic rotational inversions, it suggests that the principle mechanism responsible for maintaining the solar meridional circulation is the inertia of the differential rotation, as represented by the Coriolis force (§2.2).

Together with these three physical premises, we use three observational foundations. The first is the solar differential rotation inferred from helioseismology. The second is a persistent poleward meridional flow from low to high latitudes for  $r \gtrsim 0.95R$  with an amplitude of roughly  $10\text{--}15\text{ m s}^{-1}$ . The third observational foundation is the mean density profile  $\rho(r)$  in the CZ. Although this is obtained from a solar structure model (Model S), we regard it as an observation because it is verified to within a few percent by helioseismic structure inversions.

The results suggest that the amplitude of convective velocities in the upper CZ ( $r \sim 0.95R$ ) must be at least  $30\text{ m s}^{-1}$  in order to sustain the observed mean flows. Analogous limits in the lower CZ are less reliable due to uncertainties about the meridional flow but reasonable inferences suggest that convective amplitudes can be no less than about  $8\text{ m s}^{-1}$  at  $r \sim 0.75$ .

The existence of the near-surface shear layer (NSSL) provides a smoking gun that we can exploit to link these convective amplitudes to a size scale. In particular, it suggests that the characteristic Rossby number crosses unity somewhere near the base of the NSSL at

$r \sim 0.95R$  (MH11). Together with the velocity limits obtained in §3, this implies deeper convective motions can be no smaller than 5.5 Mm. This is of course a conservative limit. Surface convection simulations suggest that the size scale of convective motions progressively increases with depth, from the  $\sim 1$  Mm granulation scales at the surface to  $\sim 30$  Mm supergranulation scales by  $r \sim 0.97R$ , due mainly to an increase in the density and pressure scale heights (e.g. Rempel 2011; Trampedach & Stein 2011). Still, the limit given here provides an independent constraint on the size of deep convection that depends only on the three physical premises and observational foundations noted above (along with a fourth premise that  $R_o \lesssim 1$  marks the base of the NSSL).

The lower limits on convective velocity and size scales reported here are consistent with the upper limits inferred from local helioseismology by Hanasoge et al. (2010) provided that the characteristic size of the convective motions at  $r \sim 0.95R$  lies somewhere in the range between 5.5–83 Mm. This corresponds to a range in spherical harmonic degree of  $50 \lesssim \ell \lesssim 750$ . This range may be too wide to provide a strong constraint on convection models but it can be narrowed somewhat if one requires that motions at and below  $r \sim 0.95R$  be no smaller than supergranules, so  $L_c \gtrsim 30$  Mm and  $\ell \lesssim 130$ .

Since our work is concerned specifically with the relationship between convective transport and mean flows, it has important implications for Flux Transport dynamo models (§4.3). In particular, it suggests that advection-dominated FT models are not self-consistent in the sense that the assumed magnitude of convective transport is generally too low to account for the mean flows they require to operate. This has been argued before based on estimates of  $V_c$  and  $L_c$  obtained from mixing length theory and convection models (cf. Fig 3). However, here we demonstrate that it is a more general consequence of the need to sustain the mean flows against their own inertia.

The essence of the problem can be appreciated simply from Eq. (8). If  $(2\delta)^{1/2} \sim 1$  and  $V_\Omega \gg V_m$ , then  $V_c$

must be significantly larger than  $V_m$ . Thus, one would expect convection to dominate transport over the meridional circulation unless its spatial and temporal correlation scales are small. However, these correlation scales cannot be too small because if they were, the influence of rotation on the convection would not be strong enough to establish a solar-like differential rotation (i.e.  $R_o$  would be greater than unity; see §4.1).

This result casts some doubt on the advection-dominated flux-transport paradigm as a viable model of the solar cycle but it does not necessarily rule it out. An alternative possibility is that convective flux transport in the extreme parameter regimes of the solar interior is much less efficient than suggested by turbulent diffusion and that we have much to learn about reliably representing this transport in mean-field dynamo models.

The estimates reported here are independent of mixing-length theory and convection simulations but they give compatible values for  $V_c$  and  $L_c$ , suggesting internal consistency (§4.2). Furthermore, they suggest that the velocity and length scales responsible for maintaining solar mean flows cannot be drastically different from those currently exhibited by global convection simulations. This bodes well for the future; as global convection models continue to move toward higher resolution and improved representations of the upper and lower boundary layers, they should be able to capture the essential physics underlying the solar differential rotation and meridional circulation with increasing fidelity.

We thank Yuhong Fan and Bidya Karak for comments on the manuscript and the anonymous referee for constructive criticisms that have improved the presentation. We also thank Rachel Howe for providing the rotational inversions used to construct Fig. 2, and Kyle Augustson, Ben Brown, Nick Nelson, and Juri Toomre for many enlightening and inspiring discussions. This work is supported by NASA grants NNN09AK14I (Heliophysics SR&T) and NNX08AI57G (Heliophysics Theory Program). The National Center for Atmospheric Research is sponsored by the National Science Foundation.

## REFERENCES

- Augustson, K., Rast, M., Trampedach, R., & Toomre, J. 2011, *J. Phys. Conf. Ser.*, 271, 012070
- Aurnou, J., Heimpel, M., & Wicht, J. 2007, *Icarus*, 190, 110
- Balbus, S. A., Bonart, J., Latter, H. N., & Weiss, N. O. 2009, *MNRAS*, 400, 176
- Balbus, S. A. & Schaan, E. 2012, *The Stability of Stratified, Rotating Systems and the Generation of Vorticity in the Sun*, in preparation
- Basu, S. & Antia, H. M. 2010, *ApJ*, 717, 488
- Beck, J. G., Gizon, L., & Duvall, T. L. 2002, *ApJ*, 575, L47
- Bonanno, A., Elstner, D., Rüdiger, G., & Belvedere, G. 2002, *Astron. Astrophys.*, 390, 673
- Braun, D. C. & Fan, Y. 1998, *ApJ*, 508, L105
- Brun, A. S., Miesch, M. S., & Toomre, J. 2004, *ApJ*, 614, 1073
- . 2011, *ApJ*, 742, 79 (20pp)
- Brun, A. S. & Toomre, J. 2002, *ApJ*, 570, 865
- Busse, F. H. 2002, *Phys. Fluids*, 14, 1301
- Charbonneau, P. 2010, *Living Reviews in Solar Physics*, 7, <http://www.livingreviews.org/lrsp-2010-3>
- Chou, D.-Y. & Dai, E.-C. 2001, *ApJ*, 559, L175
- Choudhuri, A. R., Schüssler, M., & Dikpati, M. 1995, *Astron. Astrophys.*, 303, L29
- Christensen-Dalsgaard, J. 2002, *Rev. Mod. Phys.*, 74, 1073
- Christensen-Dalsgaard, J. et al. 1996, *Science*, 272, 1286
- DeRosa, M. L., Gilman, P. A., & Toomre, J. 2002, *ApJ*, 581, 1356
- DeRosa, M. L. & Toomre, J. 2004, *ApJ*, 616, 1242
- Dikpati, M. & Charbonneau, P. 1999, *ApJ*, 518, 508
- Dikpati, M. & Gilman, P. A. 2001, *ApJ*, 559, 428
- . 2006, *ApJ*, 649, 498
- . 2009, *Space Sci. Rev.*, 144, 67
- Eliassen, A. 1951, *Astrophysica Norvegica*, V, 19
- Featherstone, N. A., Miesch, M. S., & Brown, B. P. 2012, in preparation
- Garaud, P. & Arreguin, L. A. 2009, *ApJ*, 704, 1
- Giles, P. M., Duvall, T. L., Scherrer, P. H., & Bogart, R. S. 1997, *Nature*, 390, 52
- Gilman, P. A. 1977, *Geophys. Astrophys. Fluid Dyn.*, 8, 93
- Gilman, P. A. & Foukal, P. V. 1979, *ApJ*, 229, 1179
- González-Hernández, I., Komm, R., Hill, F., Howe, R., Corbard, T., & Haber, D. A. 2006, *ApJ*, 638, 576
- Gough, D. O. & McIntyre, M. E. 1998, *Nature*, 394, 755
- Guerrero, G., Dikpati, M., & de Gouveia Dal Pino, E. 2009, *ApJ*, 701, 725
- Hanasoge, S. M., Duvall, T., & DeRosa, M. L. 2010, *ApJ*, 712, L98
- Hanasoge, S. M., Duvall, T., & Sreenivasan, K. R. 2012, *Anomalous Weak Solar Convection*, *proc. Nat. Acad. Sci.*, doi:10.1073/pnas.1206570109

- Hathaway, D. H. 1982, *Solar Phys.*, 77, 341  
—, 2011, The Sun's Shallow Meridional Circulation, arXiv:1103.1561
- Hathaway, D. H., Beck, J. G., Bogart, R. S., Bachmann, K. T., Khatri, G., Petitto, J. M., Han, S., & Raymond, J. 2000, *Solar Physics*, 193, 299
- Hathaway, D. H. & Rightmire, L. 2010, *Science*, 327, 1350
- Haynes, P. H., Marks, C. J., McIntyre, M. E., Shepherd, T. G., & Shine, K. P. 1991, *J. Atmos. Sci.*, 48, 651
- Hotta, H. & Yokoyama, T. 2010, *ApJ*, 714, L308
- Howe, R., Christensen-Dalsgaard, J., Hill, F., Komm, R. W., Larsen, R. M., Schou, J., Thompson, M. J., & Toomre, J. 2000, *Science*, 287, 2456
- Isik, E. & Holzwarth, V. 2009, *A&A*, 508, 979
- Jiang, J., Chatterjee, P., & Choudhuri, A. R. 2007, *MNRAS*, 381, 1527
- Jouve, L. & Brun, A. 2007, *Astron. Astrophys.*, 474, 239
- Karak, B.B. 2010, *ApJ*, 724, 1021
- Kitchatinov, L. L. & Rüdiger, G. 1995, *A&A*, 299, 446  
—, 2005, *Astron. Nachr.*, 326, 379
- Küker, M., Rüdiger, G., & Schultz, M. 2001, *Astron. Astrophys.*, 374, 301
- McIntyre, M. E. 1998, *Prog. Theor. Phys. Supl.*, 130, 137, corrigendum, *Prog. Theor. Phys.*, 101, 189 (1999).
- Miesch, M. S. 2005, *Living Reviews in Solar Physics*, 2, <http://www.livingreviews.org/lrsp-2005-1>
- Miesch, M. S., Brun, A. S., DeRosa, M. L., & Toomre, J. 2008, *ApJ*, 673, 557
- Miesch, M. S., Brun, A. S., & Toomre, J. 2006, *ApJ*, 641, 618
- Miesch, M. S. & Hindman, B. W. 2011, *ApJ*, 743, 79 (25pp)
- Miesch, M. S. & Toomre, J. 2009, *Ann. Rev. Fluid Mech.*, 41, 317
- Munoz-Jaramillo, A., Nandy, D., & P.C.H.Martens. 2009, *ApJ*, 698, 461  
—, 2011, *ApJ*, 727, L23 (6pp)
- Nandy, D. & Choudhuri, A. R. 2001, *ApJ*, 551, 576
- Rast, M. P., Ortiz, A., & Meisner, R. W. 2008, *ApJ*, 673, 1209
- Read, P. 1986, *Quart. J. R. Met. Soc.*, 112, 253
- Rempel, M. 2005, *ApJ*, 622, 1320  
—, 2006, *ApJ*, 647, 662  
—, 2011, *ApJ*, 740, 15 (18pp)
- Rempel, M., Schüssler, M., & Knölker, M. 2009, *ApJ*, 691, 640
- Robinson, F. J. & Chan, K. L. 2001, *MNRAS*, 321, 723
- Roudier, T., Rieutord, M., Malherbe, J., Renon, N., Berger, T., Frank, Z., Prat, V., Gizon, L., & Svanda, M. 2012, *Astron. Astrophys.*, 540, A88
- Schou, J., Howe, R., Basu, S., Christensen-Dalsgaard, J., Corbard, T., Hill, F., Komm, R., Larsen, R. M., Rabello-Soares, M. C., & Thompson, M. J. 2002, *ApJ*, 567, 1234
- Spiegel, E. A. & Zahn, J.-P. 1992, *Astron. Astrophys.*, 265, 106
- Tassoul, J. L. 1978, *Theory of Rotating Stars* (Princeton: Princeton Univ. Press)
- Thompson, M. J., Christensen-Dalsgaard, J., Miesch, M. S., & Toomre, J. 2003, *ARA&A*, 41, 599
- Trampedach, R. & Stein, R. F. 2011, *ApJ*, 731, 78 (7pp)
- Ulrich, R. K. 2010, *ApJ*, 725, 658
- Vögler, A., Shelyag, S., Schüssler, M., Cattaneo, F., Emonet, T., & Linde, T. 2005, *Astron. Astrophys.*, 429, 335
- Wang, Y. M., Sheeley, N. R., & Nash, A. G. 1991, *ApJ*, 383, 431
- Weber, M. A., Fan, Y., & Miesch, M. S. 2011, *ApJ*, 741, 11 (14pp)
- Yeates, A. R., Nandy, D., & Mackay, D. H. 2008, *ApJ*, 673, 544

## APPENDIX

### *Baroclinicity as a Source of Differential Rotation*

In §2.2 we argued that baroclinic forcing cannot account for the observed sense of the solar meridional flow (poleward near the surface). In this Appendix we demonstrate further that baroclinicity alone cannot account for the solar differential rotation as inferred from helioseismology. Similar issues have been studied for decades within the context of planetary and stellar atmospheres (Eliassen 1951; Read 1986; Tassoul 1978).

The importance of baroclinicity for shaping the solar differential rotation profile is undisputed. Theoretical models, mean-field models, and global convection simulations all suggest that baroclinic forcing is necessary to account for the conical nature of mid-latitude  $\Omega$  surfaces in the solar CZ inferred from helioseismology (Kitchatinov & Rüdiger 1995; Robinson & Chan 2001; Brun & Toomre 2002; Rempel 2005; Miesch et al. 2006; Balbus et al. 2009). However, this result should not be misinterpreted to attribute the solar differential rotation entirely to baroclinic forcing.

Such a clarification is particularly timely in light of the recent work by Balbus & Schaen (2012). They demonstrate that the centrifugal distortion of the base of the convection zone can produce thermal gradients along isobaric surfaces that can in turn induce differential rotation through baroclinic forcing. This background shear may then interact with convection to produce the observed mean flows. We do not dispute this argument but again we caution against a potential misinterpretation of their results. In particular, we argue that baroclinicity alone cannot induce a net equatorward angular velocity gradient ( $\partial\Omega/\partial\theta > 0$  in the northern hemisphere, or NH) throughout the CZ as exhibited by helioseismic rotational inversions.

Our argument begins with the time-dependent zonal vorticity equation (4). Again we neglect the Reynolds stress, Lorentz force, and viscous diffusion. We proceed to consider a fixed entropy gradient  $\partial\langle S\rangle/\partial\theta$  and we ask what differential rotation such baroclinic forcing will produce when subject to a given initial condition  $\Omega(r, \theta, t = 0) = \Omega_i(r, \theta)$  and  $\mathbf{v}_m(t = 0) = 0$ .

As noted in §2.2, a poleward entropy gradient will induce a clockwise meridional circulation cell in the NH ( $\partial\langle S\rangle/\partial\theta < 0$ ,  $\langle\omega_\phi\rangle > 0$ ). Although it was not necessary for the arguments presented in §2, we now adopt the anelastic approximation so the mean mass flux is divergenceless:

$$\nabla \cdot \langle \bar{\rho} \mathbf{v}_m \rangle = 0 \quad (1)$$

where  $\bar{\rho}(r)$  is the background density profile, averaged over latitude, longitude, and time. Thus, the conservation of mass requires that the generation of zonal vorticity  $\langle\omega_\phi\rangle$  be associated with flows both toward and away from the rotation axis. This is crucial in understanding the significance of the results that follow.

In order to address the generation of rotational shear, we must consider the time-dependent version of the zonal momentum Eq. (1). Another crucial realization required to appreciate the results that follow is that there is no baroclinic component of the net axial torque  $\mathcal{F}$ . Recall that  $\mathcal{F}$  involves only the Reynolds stress, the Lorentz force, and the viscous diffusion (explicit expressions are given in MH11). If baroclinic forcing is to induce a differential

rotation, it must do so by means of the meridional flow. Thus, we can set  $\mathcal{F} = 0$ , which yields (MH11)

$$\bar{\rho} \frac{\partial \mathcal{L}}{\partial t} = - \langle \bar{\rho} \mathbf{v}_m \rangle \cdot \nabla \mathcal{L} \quad . \quad (2)$$

In Eq. (2) we have again used the anelastic approximation so we have replaced  $\rho$  with  $\bar{\rho}$ .

Two things are immediately apparent from Eq. (2). First, for a given meridional flow  $\langle \bar{\rho} \mathbf{v}_m \rangle$ , this is identical to the equation for passive advection of a scalar field. Second, the only steady solution is one in which  $\langle \bar{\rho} \mathbf{v}_m \rangle \cdot \nabla \mathcal{L} = 0$ . Such a steady state can be achieved in one of two ways. Either the meridional flow must vanish  $\langle \mathbf{v}_m \rangle = 0$  or the specific angular momentum  $\mathcal{L}$  must be constant on streamlines. The latter case,  $\mathcal{L} = \lambda^2 \Omega$  constant on streamlines, would necessarily be associated with an anti-solar differential rotation profile, such that the poles would spin faster than the equator ( $\partial \Omega / \partial \theta < 0$  in the NH). We will return to the former case, that of  $\langle \mathbf{v}_m \rangle = 0$  below.

Now return the time-dependent problem outlined above in which we follow the response of the mean flows to a specified baroclinic forcing  $\partial \langle S \rangle / \partial \theta$ . Let us assume for simplicity that the initial angular velocity profile is cylindrical, so  $\Omega_i = \Omega_i(\lambda)$ . As noted below, this is not a necessary assumption but it serves well to illustrate the main point. Furthermore, we will assume that the initial angular momentum gradient is directed away from the rotation axis, so  $d\mathcal{L}_i/d\lambda > 0$ , where  $\mathcal{L}_i = \lambda^2 \Omega_i$ . This is true for the current Sun, it is true for a uniform rotation ( $\Omega_i = \Omega_0$ ), and we suspect that it is true in general for stars since the alternative,  $d\mathcal{L}_i/d\lambda < 0$  is unstable according to the Rayleigh criterion (Tassoul 1978). Note that the case  $\nabla \mathcal{L} = 0$  is a fixed point; if this were the initial state, meridional circulation would not influence the zonal flow and baroclinicity would not induce a differential rotation.

Consider a volume  $\mathcal{V}$  defined by  $r \leq R$  and  $\lambda \leq \lambda_0$ , where  $R$  is the solar surface and  $\lambda_0$  is a fiducial cylindrical radius that can lie anywhere between zero and  $R$ . Integrating Eq. (2) over  $\mathcal{V}$  and using Eq. (1) yields

$$\frac{dL_{\mathcal{V}}}{dt} = \int_{\mathcal{S}} \mathcal{L} \langle \bar{\rho} \mathbf{v}_m \rangle \cdot d\mathbf{S} = 2\pi\lambda \int_{z_-}^{z_+} \mathcal{L} \langle \bar{\rho} v_{\lambda} \rangle dz \quad (3)$$

where

$$L_{\mathcal{V}} = \int_{\mathcal{V}} \bar{\rho} \mathcal{L} dV \quad (4)$$

is the total angular momentum within  $\mathcal{V}$  and  $z_{\pm} = \pm(R^2 - \lambda_0^2)^{1/2}$ . We have assumed that there is no flow across  $r = R$ .

At the initial time  $t = 0$  the  $\Omega$  profile is cylindrical so  $\mathcal{L}$  can be pulled out of the integral on the right-hand-side (RHS). Mass conservation then implies that the RHS vanishes and the rate of change of  $L_{\mathcal{V}}$  vanishes. However, the analogy with the passive scalar noted above makes it clear that this cannot hold indefinitely. Our intuition tells us that if  $d\mathcal{L}_i/d\lambda > 0$  then the advection of angular momentum into our volume must increase  $L_{\mathcal{V}}$  over time.

This apparent inconsistency can be resolved if we consider a Taylor expansion at early times

$$L_{\mathcal{V}}(t) = L_{\mathcal{V}}(0) + t \left. \frac{dL_{\mathcal{V}}}{dt} \right|_{t=0} + t^2 \left. \frac{d^2 L_{\mathcal{V}}}{dt^2} \right|_{t=0} + \dots \quad (5)$$

Applying a time derivative to (3) and substituting in (2) yields

$$\left. \frac{d^2 L_{\mathcal{V}}}{dt^2} \right|_{t=0} = 2\pi\lambda \int_{z_-}^{z_+} \langle \bar{\rho} v_{\lambda} \rangle \frac{\partial \mathcal{L}}{\partial t} dz = 2\pi\lambda \int_{z_-}^{z_+} \bar{\rho} \langle v_{\lambda} \rangle^2 \frac{d\mathcal{L}_i}{d\lambda} dz \quad . \quad (6)$$

In obtaining this result we have neglected the time dependence of  $\langle \mathbf{v}_m \rangle$ . Thus, the second derivative of  $L_{\mathcal{V}}$  is positive definite at  $t = 0$ . Together with (5) this implies that the angular momentum within  $\mathcal{V}$  will increase with time.

Put another way, this implies that any persistent meridional circulation will tend to spin up the poles relative to the equator. This is true regardless of the (nonzero) amplitude or profile of the circulation and regardless of the source of the circulation, whether it be baroclinic in nature or due to some other meridional forcing. Furthermore, it holds for any arbitrary initial  $\mathcal{L}$  profile that is stable in the sense that  $\partial \mathcal{L}_i / \partial \lambda > 0$ . In this general case,  $\mathcal{L}$  surfaces would still intersect  $R$  at two locations and  $\mathcal{V}$  would be defined relative to the surface  $\mathcal{L} = \mathcal{L}_0$  such that  $r \leq R$  and  $\mathcal{L} \leq \mathcal{L}_0$ . Then Eq. (6) would still hold with  $d\mathcal{L}_i/d\lambda$  replaced by  $|\nabla \mathcal{L}| \cdot \langle v_{\lambda} \rangle^2$  by  $(\langle \mathbf{v}_m \rangle \cdot \hat{\mathbf{n}})^2$  (where  $\hat{\mathbf{n}}$  is the unit vector normal to  $\mathcal{S}$ ) and the integration would proceed over the surface  $\mathcal{S}$ . The early time dependence would still be given by (5) with  $(dL_{\mathcal{V}}/dt)_{t=0} = 0$  and  $(d^2 L_{\mathcal{V}}/dt^2)_{t=0} > 0$ .

This argument can also be readily generalized to a spherical annulus. If there is a radius  $r_b$  below which the meridional flow  $\langle \mathbf{v}_m \rangle$  becomes negligible, then one can define the volume  $\mathcal{V}$  to be bounded from above and below by  $R$  and  $r_b$ , extending poleward of an  $\mathcal{L}$  isosurface that extends from  $R$  to  $r_b$  (confined either to the northern or southern hemisphere). Then the conclusion is unaltered; a baroclinically-driven meridional flow will increase the total angular momentum in the polar cap  $\mathcal{V}$  over time, provided only that  $\partial \mathcal{L}_i / \partial \lambda > 0$ .

Spin-up of the poles can be avoided if the Rossby number is small, which is a good approximation for the Sun. Here the relevant Rossby number is that based on the meridional flow  $R_o^m = V_m / (2\Omega_0 R)$ . For  $R_o^m \ll 1$ , meridional flows are redirected into zonal flows essentially immediately (on the time scale of a rotation period), so the steady-state version of Eq. (2) can be satisfied with  $\langle \mathbf{v}_m \rangle = 0$ . At the same time, a differential rotation will be quickly established that obeys thermal wind balance, Eq. (5).



This is indeed a viable way to generate an axial shear  $\partial\Omega/\partial z$  and may play an important role in the Sun. However, it cannot spin up the equator relative to the poles, as seen in the solar convection zone. In the limit  $R_o^m \ll 1$ , there is no angular momentum transport across  $\lambda$  surfaces. Rather, at a given cylindrical radius  $\lambda$ , any deceleration of  $\Omega$  for some range of  $z$  must be balanced by an acceleration at some other  $z$ . This follows directly from the conservation of mass and angular momentum as outlined above.

This implies that a solar-like differential rotation characterized by an equatorward  $\nabla\Omega$  in the CZ can only be produced by baroclinic forcing if there is a corresponding poleward  $\nabla\Omega$  somewhere below the CZ. We cannot rule this out from helioseismic rotational inversions but there is currently no evidence for it.

We emphasize that the thermal wind equation (5) possesses a geostrophic degeneracy in that a given entropy gradient  $\partial\langle S\rangle/\partial\theta$  is compatible with an infinite number of  $\Omega$  profiles, some solar-like ( $\partial\Omega/\partial\theta > 0$  in the NH) and some anti-solar. This arises because one can take a solution of this equation  $\Omega_s(r, \theta)$  and add an arbitrary cylindrical component  $\Omega'(\lambda)$  and the sum is also a solution. We argue that the convective Reynolds stress is necessary to break this degeneracy and establish a solar-like  $\Omega$  profile.

In any case, it is clear that there must be some non-baroclinic forcing in the solar CZ in order to account for the observed mean flows. As noted in §1, solar observations indicate a persistent poleward circulation in the solar surface layers and mass conservation requires a net equatorward flow deeper down. Since  $\mathcal{L}$  isosurfaces are nearly cylindrical throughout the CZ (MH11), this necessarily implies flow across  $\mathcal{L}$  contours that must be balanced in a steady state with a nonzero  $\mathcal{F}$ , as expressed in Eq. (1).